Fisheries and Oceans Canada | Pêches et Océans Canada
Science | Sciences

Canadian Science Advisory Secretariat (CSAS)

Research Document 2014/049

Québec Region

Chemical and Biological Oceanographic Conditions in the Estuary and Gulf of St. Lawrence during 2011 and 2012

S. Plourde, M. Starr, L. Devine, J.-F. St-Pierre, L. St-Amand, P. Joly, and P. S. Galbraith

Fisheries and Oceans Canada, Québec Region
Maurice Lamontagne Institute
850 de la Mer, P. O. Box 1000
Mont-Joli, QC G5H 3Z4

September 2014

Canada

Foreword

This series documents the scientific basis for the evaluation of aquatic resources and ecosystems in Canada. As such, it addresses the issues of the day in the time frames required and the documents it contains are not intended as definitive statements on the subjects addressed but rather as progress reports on ongoing investigations.

Research documents are produced in the official language in which they are provided to the Secretariat.

Published by:

Fisheries and Oceans Canada
Canadian Science Advisory Secretariat
200 Kent Street
Ottawa ON K1A 0E6

http://www.dfo-mpo.gc.ca/csas-sccs/
csas-sccs@dfo-mpo.gc.ca

© Her Majesty the Queen in Right of Canada, 2014
ISSN 1919-5044

Correct citation for this publication:

S. Plourde, Starr, M., Devine, L., St-Pierre, J.-F., St-Amand, L., Joly, P., and Galbraith, P. S. 2014. Chemical and biological oceanographic conditions in the Estuary and Gulf of St. Lawrence during 2011 and 2012. DFO Can. Sci. Advis. Sec. Res. Doc. 2014/049. v + 46 pp.

TABLE OF CONTENTS

BSTRACT iv
ÉSUMÉ v
TRODUCTION 1
ETHODS 1
ESULTS 4
Nutrients and phytoplankton 4
Fixed stations 4
Sections and late-winter helicopter survey 5
Remote sensing of ocean colour 6
Zooplankton 7
Fixed stations 7
Sections 8
Copepod phenology 9
Scorecards 9
SCUSSION 10
JMMARY 13
CKNOWLEDGEMENTS 14
EFERENCES 14

ABSTRACT

ocument reports on the chemical and biological conditions in the Gulf of St. Lawrence for 2011 and 2012 in the context of a strong warming event that began in 2008. Data ese two years are compared to time-series observations starting in 1999. Zooplankton and the spatial scales considered were modified from previous reports to match more those of other regions involved in the Atlantic Zone Monitoring Program (AZMP). All lankton and zooplankton abundance indices and nutrient inventories were relatively nt through the time series (1999–2012) among fixed stations, sections, and large ions. Winter, spring, and fall surface nitrate inventories have been below the normal 010 in many regions of the Gulf. A shift to earlier timing of the spring bloom has also bserved since 2010 across many of the Gulf subregions. In addition, chlorophyll levels late spring, summer, and fall have tended to be predominately below normal since 2010. s evidence of ontogenetic and phenological changes in *Calanus* species that appear to direct effects of the warmer environmental conditions experienced by the region over the v years. High abundances of large-bodied arctic and subarctic species occurring neously with the near-record high surface temperature in 2012 suggest that these s avoid or adapt their life cycle strategy to minimize potential negative effects of warm ons in the surface layer. At the same time, an increased abundance of warm-water s was observed. High abundances of cold/arctic species concomitant with those of warm-pecies likely reflect the complex hydrography of the GSL system and highlight the Gulf's n as a transitional zone between the "upstream" Labrador/Newfoundland shelf and the tream" Scotian Shelf.

ons océanographiques chimiques et biologiques dans l'estuaire et le golfe du Saint-Laurent en 2011 et 2012

RÉSUMÉ

ort documente les résultats concernant les conditions biologiques dans de golfe du St-
en 2011 et 2012 dans le contexte d'un réchauffement significatif des températures
n 2008. Les données de 2011 et 2012 sont comparées à celles de la série temporelle
cée en 1999. Les indices du zooplancton ainsi que les échelles spatiales utilisées ont
fiés afin de mieux refléter la structure des autres rapports du Programme de
ge zonal atlantique (PMZA) des autres régions. Tous les indices de nutriments et
nce du phytoplancton et zooplancton pour les stations fixes, les transects et les
régions sont cohérents tout le long de la série temporelle (1999–2012). Les niveaux de
surface au cours de l'hiver, du printemps et de l'automne tendent être en dessous de
le depuis 2010 dans de nombreuses régions du Golfe du Saint-Laurent. Un
ent à la précocité de la floraison printanière est aussi évident dans plusieurs sous-
lu golfe du Saint-Laurent depuis 2010. De plus, les concentrations de chlorophylle à la
ntemps, au cours de l'été et de l'automne ont tendance à être essentiellement en
de la normale depuis 2010. On observe aussi des changements clairs dans l'ontogénie
nologie des espèces de *Calanus* qui semblent être causées par des conditions
ementales se réchauffant dans la région depuis quelques années. Les abondances
des espèces de gros copépodes arctiques et subarctiques observées simultanément
t que ces espèces pourraient adapter leur stratégie de cycle de vie afin de minimiser
négatifs de conditions plus chaudes dans les eaux de surface. Dans le même temps,
mentation de l'abondance des espèces d'eaux chaudes a été observée. La présence
ée d'espèces d'eaux froides et d'eaux chaudes reflète la complexité hydrographique du
St-Laurent et montre que ce dernier est positionné comme une zone de transition entre
nordiques du Labrador/Terre Neuve et les eaux plus chaudes du plateau néo-

INTRODUCTION

ic Zone Monitoring Program (AZMP) was implemented in 1998 (Therriault et al. 1998) m of (1) increasing the Department of Fisheries and Oceans' (DFO's) capacity to d, describe, and forecast the state of the marine ecosystem and (2) quantifying the the ocean's physical, chemical, and biological properties and the predator–prey ps of marine resources. A critical element in the observational program of AZMP is an sessment of the distribution and variability of nutrients and the plankton they support.

on of the spatiotemporal distribution of nutrients (nitrate, silicate, phosphate) and ssolved in seawater provides important information on water-mass movements and on ns, timing, and magnitude of biological production cycles. A description of the of phytoplankton and zooplankton provides important information on the organisms e base of the marine food web. An understanding of plankton production cycles is an art of an ecosystem approach to fisheries management.

derives its information on the state of the marine ecosystem from data collected at a sampling locations (fixed-point stations, cross-shelf sections) in each DFO region Gulf, Maritimes, Newfoundland; see Fig. 1 for Québec and Gulf region locations) t a frequency of twice-monthly to once annually. The sampling design provides basic on the natural variability in physical, chemical, and biological properties of the Atlantic continental shelf. Cross-shelf sections provide detailed geographic but are limited in their seasonal coverage. Critically placed fixed stations nt the geography-based sampling by providing more detailed information on temporal changes in ecosystem properties.

ument, we review the chemical and biological oceanographic (lower trophic levels) in the Québec region in 2011 and 2012. During these years, surface water re and other physical indices showed strong anomalies indicative of a much warmer nt than during the previous decade (Galbraith et al. 2013). In particular, 2012 was zed by record-high surface temperatures from mid-summer to fall and a strong ep-water temperature anomaly. In addition, we saw near-historical values in the cold te layer (CIL; low volume / high minimum temperature index) and in ice conditions e and duration) (Galbraith et al. 2013). Water temperatures were also at record or d highs in the other AZMP regions (DFO 2013). In the context of these unusually litions in 2011 and 2012, this report aims to describe changes in the annual cycles and community composition of phytoplankton and zooplankton.

METHODS

collection and processing steps meet and often exceed the standards of the AZMP Mitchell et al. 2002). All data included in this report were collected along seven uring the missions in June and October–November of each year and at the four fixed ig. 1). Table 1 and Figure 2 show the 2011 and 2012 missions and fixed stations requencies, respectively. The Gaspé Current (GC), Anticosti Gyre (AG), and Shediac d stations were visited less frequently than planned in 2011 and 2012 (Table 1, ile Rimouski station was sampled at roughly weekly intervals from early spring to late w sampling frequency at GC and AG is the result of a lack of vessel availability, in winter.

sampling was accomplished during a survey of the winter surface mixed layer of the Lawrence (GSL) and of the surface nutrients (2 m); this survey has taken place in

-March since 1996 (2002 for nutrients) using a Canadian Coast Guard helicopter. ded a considerable amount of data to the previously very sparse winter sampling in The survey and sampling methods are described in Galbraith (2006) and in Galbraith . A total of 93 stations were sampled during the 8–17 March 2011 survey and 106 –17 March 2012 survey. The temperature and salinity of the 2011 and 2012 mixed escribed by Galbraith et al. (2012, 2013).

e phytoplankton biomass was estimated from ocean colour data collected by the Wide Field-of-view Sensor (SeaWiFS) satellite launched by NASA in late summer the Moderate Resolution Imaging Spectroradiometer (MODIS) "Aqua" sensor NASA in July 2002. Because the SeaWIFS mission ended in December 2010, we e the MODIS data obtained continuously from January 2003 until December 2012 to mposite time series of surface chlorophyll *a* in six GSL subregions (Anticosti Gyre, hallows, Shediac Valley, Cabot Strait, northwest and northeast Gulf of St. ee Fig. 3 for locations). Because data for the estuarine portion of the Gulf are lue to turbidity and riverine input of terrestrially derived coloured matter), we regions outside of the St. Lawrence River plume. Composite satellite images were IO's remote sensing unit (DFO, Dartmouth, NS) in collaboration with NASA GSFC. ics (mean, range, standard deviation) are extracted from two-week average with a 1.5 km spatial resolution. Seven different metrics were computed using posite data: the timing of spring bloom start and peak (day of year); the magnitude bloom (maximum chlorophyll *a*); and the chlorophyll *a* mean during spring (March mmer (June to August), and fall (September to December) as well as the annual arch to December). In addition, we computed normalized annual anomalies (see ach of the different bloom metrics to evaluate evidence of temporal trends among statistical subregions.

and nutrient data collected along the AZMP sections and at fixed stations were ver various depth intervals (i.e., 0–10 m for chlorophyll; 0–5 m and 50–15 m for ing trapezoidal numerical integration. The surface (0 m) data were actually the ampled values; data at the lower depths were taken as either i) the interpolated sampling was below the lower integration limit or ii) the closest deep-water sampled sampling was shallower than the lower integration limit. Integrated nitrate values copter survey were calculated using surface concentrations (2 m) × 50 m hat the nitrate concentrations are homogeneous in the winter mixed layer at that ear).

ankton data collected in 2000 and 2001 along the AZMP sections and fixed stations ed from the present analysis because of serious doubts about the quality of the y are being re-analyzed in 2013–2014). In this document, the detailed description patterns in zooplankton indices was restricted to the Rimouski and Shediac fixed to the very low sampling frequency at GC and AG in 2011 and 2012 (Table 1). ta from these sites were included in figures to allow comparisons of the seasonal bserved at each site and to complement some observations. Finally, we present l climatologies of zooplankton biomass and total copepodite abundance of *Calanus* and *C. hyperboreus* at Rimouski station for two depth layers (0–100 m, 100– 2005 to 2010 (see Perrin et al. 2014 for the methodology) to assess the of the fixed sites in quantifying different components of the zooplankton community.

previous research documents reporting on conditions in the GSL, the number and lankton indices as well as the way they are reported have been rationalized as a ard standardization with research documents from other AZMP regions. We e presentation of results from the fixed sites to total zooplankton biomass, total

ndance, relative contribution of the 10 most abundant copepod species, and *C.* and *Pseudocalanus* spp. abundance and stage composition. Because of its the total zooplankton biomass in the region, a detailed description of *C.* was added. Total zooplankton biomass is the only index presented for the seven AZMP sections. We also wished to report GSL results at a spatial scale similar to ther regions, so the annual averaged total zooplankton biomass and total *C. finmarchicus*, *C. hyperboreus,* and *Pseudocalanus* spp. were calculated for having distinct oceanographic regimes (Koutitonsky and Budgen 1991, Galbraith

GSL (wGSL): this region is generally deep (> 200 m) and cold in summer. It is influenced by freshwater runoff from the St. Lawrence River. The wGSL includes SL, TSI, and TASO sections.

n GSL (sGSL): this region is shallow (< 100 m) and much warmer in summer. It is ne influence of the Gaspé Current. The sGSL includes the TIDM section.

GSL (eGSL): this region, with deep channels and a relatively wide shelf (< 100 haracterized by higher surface salinity and is directly influenced by the intrusion of om the Labrador and Newfoundland shelves. The eGSL includes the TDC, TCEN, B sections.

egions of the GSL correspond more to the scale addressed by AZMP in other e sampling on each section generally targets specific subregions (e.g., Grand n and western Scotian Shelf).

anomalies of key chemical and biological indices were computed for all fixed ons, and oceanographic regions. These anomalies are calculated as the ween the variable's average (for the season or for the complete year) and the rage for the reference period (usually 1999–2010); this number is then divided by period's standard deviation. These anomalies thus represent observations in a at. A standard set of indices representing anomalies of nutrient availability, biomass and bloom dynamics, and the abundance of dominant copepod species *C. finmarchicus, Pseudocalanus* spp., total copepods, and total non-copepods) are each AZMP region (see DFO 2013). In the present paper, several new ndices were also computed that reflect either different functional groups with in the ecosystem or groups of species indicative of cold- or warm-water intrusions nvironmental conditions: large calanoids (dominated by *Calanus* and *Metridia* ll calanoids (dominated by more neritic species such as *Centropages* spp., *us* spp., *Acartia* spp., *Temora* spp.), cyclopoids (dominated by *Oithona* spp. and , warm-water species (*Centropages* spp., *Paracalanus* spp., *Clausocalanus* spp.), c species (*Calanus glacialis*, *Metridia longa*).

nges in zooplankton phenology were also explored using *C. finmarchicus* as an used the time series at Rimouski station because adequate sampling and stage started there almost 20 years ago (1994). From 1994 to 2004, *C. finmarchicus* age abundance was determined using samples collected with 333 µm (CIV–CVI) I–III) mesh nets that were analyzed for seven years of the time series (see 2009 for details). In other years before 2004 for which 73 µm samples were not abundance of CI–III in the 333 µm samples was adjusted based on a comparison

ZMP-like net (S. Plourde, unpublished data[1]). The phenology of *C. finmarchicus* using the relative stage proportions of CI–III, CIV, CV, and CVI (male and se the maximum contribution of each stage is not equivalent, with CI–III and CVI enting less than 50% of total abundance while CV could be > 90% during fall, we presentation by using a common scale created by normalizing the relative ach stage: each observation was divided by its observed annual maximum

RESULTS

AND PHYTOPLANKTON

the primary dissolved inorganic nutrients (nitrate, silicate, phosphate) included in ational program strongly co-vary in space and time (Brickman and Petrie 2003). and because the availability of nitrogen is most often associated with growth limitation in coastal waters of the GSL, emphasis in this document is bility in nitrate concentrations and inventories.

s

and Shediac Valley stations typically exhibit a biologically mediated reduction in concentrations in spring/summer, a minimum during summer, and a subsequent fall/winter (Fig. 4). The onset of the nutrient draw-down occurs later at Rimouski ed to Shediac Valley, reflecting the later spring bloom in the St. Lawrence compared to Shediac Valley (April). In contrast to Shediac Valley, surface ries at Rimouski remain relatively high during summer and usually at levels non-oplankton growth. These high levels are mainly due to upwelling at the head of Channel and the high tidal mixing in this area, and to some degree to and river sources, notably from St. Lawrence River.

tion, the onset of spring nutrient draw-down in 2011 and 2012 was similar to the ming (Fig. 4). Spring, summer, and fall inventories at this station were slightly nal in 2011 but close to the long-term average in 2012. Bloom initiation occurred ge in 2011 but was somewhat later in 2012. Chlorophyll inventories were er than average in June 2011 and 2012, and an intense fall bloom was observed 012. When averaged for the entire sampling period, the chlorophyll inventories ess close to (2011) or only slightly higher than (2012) the 1999–2010 average.

hanges in phytoplankton biomass at Shediac Valley in 2011 and 2012 followed rn of high values during the spring (April–May) and low ones thereafter (Fig. 4). presence of ice in the Southern Gulf in the spring, only the later phase of the normally caught (as in 2012), or the bloom is completely missed (as in 2011) evident by the low surface nitrate inventories observed at the start of sampling. centrations were nevertheless above the average in April 2012. During the late , and fall in both 2011 and 2012, chlorophyll levels were overall below (2011) or the 1999–2010 average.

---

ceans Canada, Maurice Lamontagne Institute, 850 route de la Mer, Mont-Joli (QC), G5H

h the chlorophyll data, surface (0–50 m) nitrate inventories at Shediac station in pril–May 2012 were well below those observed during the Helicopter survey in ization by phytoplankton (Fig. 4). Low surface values persisted throughout the and 2012, and concentrations did not increase again until late fall, as has been ved. Compared to the 1999–2010 reference period, surface nutrient inventories below (2011) or close to (2012) the average.

2, diatom, dinoflagellate, and flagellate abundances were below the long-term uski station (Fig. 5). While the phytoplankton community was regularly atoms throughout the sampling period between 1999 and 2003, a shift from flagellates and dinoflagellates has been observed since 2004 (Fig. 6). The flagellates and dinoflagellates was nevertheless less pronounced in 2011 and o previous years: the diatom/flagellate and diatom/dinoflagellate ratios were 9–2010 reference period averages (Fig. 5).

ellate, and flagellate abundances at Shediac station were also below the long- xcept in 2011, when flagellate abundance was well above normal (Fig. 7). The on of the phytoplankton community composition at Shediac Valley station in as broadly similar to that seen previously, i.e., diatoms dominated during the h >75% of the total count, while flagellates and dinoflagellates dominated l count) summer (Fig. 6). However, flagellates had a higher relative abundance al during fall. In addition, the time-series anomalies revealed that the ratio at the Shediac Valley station has tended to be predominately below 9, as was observed for the Rimouski station.

ate-winter helicopter survey

2, late winter nitrate inventories were relatively high at the surface for most SL except for unusually low (<2 mmol m^{-3}) concentrations at some stations in in 2012 (Fig. 8). These atypical low levels in the southern GSL are probably l localized start of phytoplankton growth at that time of the year; this is also ite ocean colour data (see below). A similar phenomenon was observed in strong negative anomalies in the northwestern and southern GSL (Fig. 9). In he highest winter surface nitrate concentrations were observed in the St. y (SLE), and these values reached minima toward Cabot Strait and in the , as in previous years. Transport of nutrient-rich water from the Estuary hern GSL was clearly evident at that time of the year, while phytoplankton relatively weak in the system (based on satellite ocean colour data). 1, the nitrate concentrations in 2012 were especially higher in the estuarine L (SLE, northwestern GSL) and the zone under its influence (southern GSL). mpared to previous observations, the winter maximum nutrient inventories in sser degree in 2012, were below the 2002–2010 average in many areas of the (Fig. 9). This pattern appears to have begun in 2008, as revealed by the ncy of strong negative anomalies across various subregions, with the strongest es in 2010 (Fig. 10). The timing of the survey does not appear to be a factor.

pring (June) surveys of 2011 and 2012, surface nitrate inventories were low winter inventories along the seven sections crossing the Estuary and GSL due hytoplankton (Fig. 11). The depletion of nutrients in the surface layers was d in the eastern, southern, and central parts of the GSL compared to the hwestern GSL, as previously observed. During the fall 2011 and 2012 surveys, vels were comparable or only somewhat higher than those measured during rvey for most areas except for the estuarine portion of the GSL in 2012

d TASO; Fig. 11). This indicates that the autumnal turnover had not occurred n many regions.

rate inventories in 2011 and 2012 were markedly below the 1999–2010 verages for most areas of the Estuary and GSL (Fig. 10). In 2011, the en the winter maximum inventories and the late spring minimum inventories were also overall well below the 1999–2010 average while these differences ariable across the seven sections in 2012. This index represents the pool of potentially used by phytoplankton during spring. A negative index indicates ankton production rates with potential detrimental effects on higher trophic

ate inventories in 2011 and 2012 were overall below the 1999–2010 average and northwestern GSL in 2012 (Fig. 10).This may suggest that the autumnal ly delayed compared to the 1999–2010 reference period, especially in 2012. nination of the standardized scorecard anomalies reveals that spring and fall entories (similar to winter inventories) have tended to be predominately since 2010 (Fig. 10), probably reflecting the strong warming event during this

l levels in 2011 and 2012 were relatively low during the spring and fall reas of the GSL. The exceptions were the SLE and northwestern GSL along ula during the spring survey, as previously observed (Fig. 10 and 12).

g of ocean colour

our data provide large-scale images of surface phytoplankton biomass r the whole NW Atlantic. We used two-week satellite composite images of supplement our ship-based observations and provide seasonal coverage context over which to interpret our survey data. The ocean colour imagery on about the timing and spatial extent of the spring and fall blooms but does ation on the dynamics that take place below the top few metres of the water , satellite ocean colour data for the SLE are largely contaminated by high nonchlorophyllous matter originating from the continent (such as suspended loured dissolved organic matter) that render these data too uncertain to be f phytoplankton dynamics in the SLE and the subsurface information are high-frequency sampling at Rimouski station and the broad-scale veys.

2011 and 2012 revealed considerable spatial variability in the timing of the GSL (Fig. 13), as has been previously observed (not shown), which may be differences in the timing of sea-ice melt and the onset of water column uest et al. 2005). The spring phytoplankton bloom occurred between March g on the region, and started earlier in the northwest and southern parts of the MODIS imagery confirmed the initiation of the spring bloom in the southern the end of the helicopter survey in 2012 (Fig. 13). A similar phenomenon was This may explain the exceptionally low nitrate levels in this region at that time ODIS imagery also confirmed the overall low surface chlorophyll levels ur late spring and fall surveys during 2011 and 2012 (not shown). Finally, vealed that the fall blooms in the GSL in 2011 and 2012 were much weaker in ed to spring blooms, as previously observed (Fig. 14).

six GSL subregions indicate that the magnitude of surface phytoplankton the MODIS satellite was generally stronger in 2012 than in 2011

n, surface blooms occurred much earlier in many of the subregions and nger in duration in 2012 relative to the patterns noted previously. In all chlorophyll levels were extremely weak in 2012 relative to previous L. In 2011, the magnitude of surface phytoplankton bloom and the fall variable across the six statistical subregions, being either close to, 03–2010 mean.

ecard anomalies inferred from the MODIS satellite imagery showed some oss the statistical subregions (Fig. 15). A shift to earlier timing of the ally evident in the increased frequency of negative anomalies since 2010 regions. In addition, anomalies of chlorophyll levels, especially during tended to be predominately negative since 2010.

010; Rimouski: 2005–2010) seasonal climatologies of zooplankton ed stations are shown along with observations made in 2011 and 2012 in kton biomass at Rimouski station in 2011 and 2012 was slightly below above the long-term seasonal average in fall (Fig. 16a); it was also ng-term average in April–May 2012. At Shediac station, zooplankton lower than normal in May–June 2011 and near normal later in the d 2012, with only one observation well above the normal in June 2012 ese results must be considered carefully due to low sampling frequency.

ton biomass climatologies were similar for the two deep fixed stations i Gyre), with minima observed in early summer and increases to fall Examination of the seasonal climatology (2005–2010) in zooplankton species abundance in two different depth layers (0–100 m, 100–320 m) at med that deep-dwelling (>100 m) late development stages drive the eep sampling sites (Fig. 17). The seasonal climatology of zooplankton ent and Shediac stations were also alike, with low biomass in winter and ned maximum in late spring and early summer, and a much lower mer into fall (Fig. 16c, d).

relative proportions of the 10 dominant copepod species determined ll fixed sites are shown in Figures 18 and 19. Total copepod abundance July to September 2011 at Rimouski station but similar to the long-term of 2011 and throughout 2012 (Fig. 18a). This period of greater-than-ance in 2011 was associated with a greater proportion of small copepods oids) in the population; this pattern was also apparent at the other fixed The relative proportions of the 10 dominant copepod species in 2012 cross all sites, i.e., a higher proportion of large-bodied zooplankton of d *Metridia* in the population. At Gaspé Current and Shediac stations, the abundance was highly variable among sampling events, possibly an ling frequency in a region influenced by the dynamic Gaspé Current. rse sampling precluded any confident comparison with the long-term

nmarchicus was generally below the long-term average at the fixed sites 20, 21). At Rimouski station, only a few observations were above 2011 and early summer 2012 (Fig. 20a). The population stage structure

in 2011 diffe
June to Aug
first peak in
summer but
generation s
seasonal co
might have
Gaspé Curr
long-term cl

Abundance
2011 and 20
from August
Because of
sites (Fig. 2
at the Antico
similar to th
(until June)
all sampling
to be greate
developmen
sampling in
copepodite
Gyre and Ga

The fall incr
Gyre) (Fig. 1
C. finmarchi
Shediac), zo
abundance
layers of the
sampling sit
species ove
stations is d
populations

The abunda
and 2012 at
average fro
same patter
Current stat
the long-ter
stage compo
throughout t
Current stat
However, re
station in 20
on limited sa

Sections

The annual
fall surveys

long-term average, with a stronger peak in CI–III stages occurring from
a peak generally taking place in June–July (Fig. 18b, c). In 2012, a
ed during the same period as seen in the long-term climatology in early
d by a pronounced autumn peak, suggesting the production of a second
usually observed at this site (Fig. 20d). Despite a more sporadic
other fixed stations, the stage structure suggested that the CI–III peak
ier (or was shorter) in 2011 and 2012 than normal (Fig. 20g, h, 21). At
diac stations, the 2012 pattern in stage composition was similar to the
g. 21).

odied *C. hyperboreus* was near or above the long-term average in
ski station (Fig. 22). During both years, abundance was above normal
with higher abundance in April 2012 relative to April 2011 (Fig. 22).
bling, it is more difficult to describe the abundance patterns at the other
gh abundance appeared to be greater than normal in summer and fall
ion in 2012. The relative CI–III copepodite abundance was mostly
limatology, albeit with a shorter duration of CI–III in 2011 and 2012
n to the long-term average (until July) at Rimouski station (Fig. 22). At
ative proportion of CIV from July to late fall in 2011 and 2012 appeared
g-term climatology, indicating potential changes in population
ics (Fig. 22, 23). Examination of the stage structure revealed that
nd spring is critical in order to describe the recruitment period of early
species, a task rarely achieved over the last few years at Anticosti
stations (Fig. 2, 22, 23).

plankton biomass at the two deep fixed stations (Rimouski and Anticosti
associated with increased abundances of late development stages of
yperboreus (Fig. 20, 22). At the shallow stations (Gaspé Current and
omass could also be related to *C. finmarchicus* and *C. hyperboreus*
Considering the abundance patterns of *Calanus* spp. in the different
n (Fig. 17), we can conclude that zooplankton biomass at the deep
lects the zooplankton community dominated by late stages of *Calanus*
the deeper part of the GSL while zooplankton biomass at the shallow
the active components of the *C. finmarchicus* and *C. hyperboreus*
l. 2001, 2003).

calanoids (*Pseudocalanus* spp.) was strikingly different between 2011
ation (Fig. 24). In 2011, abundance was greater than the long-term
d, while it remained mostly below the normal in 2012 (Fig. 24a). The
ed to some extent at the sparsely sampled Anticosti Gyre and Gaspé
, 25a). At Rimouski station, population abundance minima similar to
ere observed from April to June in both years (Fig. 24a). Population
ged from 1999 to 2010 showed that early stages were observed
ntial for several generations) at Rimouski, Anticosti Gyre, and Gaspé
, f, 25b) (stage composition is not available for Shediac station).
early stages was restricted from late spring to September at Rimouski
this feature was observed only in 2012 at the other sites but is based
24c, d, g, h, 25c, d).

al zooplankton biomass values for each section during the spring and
Figure 26. For most sections, biomass was higher in 2012 than in

2011, with biomass in 2011 being roughly equivalent to 2010 (Fig. 26). This pattern also emerged when data are presented at a broader scale, corresponding to the three distinct oceanographic subregions, i.e., the western (wGSL), southern (sGSL), and eastern (eGSL) regions (Fig. 27). Total zooplankton biomass in the sGSL in spring showed greater interannual variability than in other GSL regions and was much higher than in fall for several years; this pattern was not observed in the wGSL or eGSL (Fig. 27). These marked differences in zooplankton biomass among years in the sGSL during the early part of the productive season could reflect interannual differences in the transport of large-bodied *Calanus* spp. from deeper adjacent regions in spring and early summer (Runge et al. 1999, Maps et al. 2010). High population loss due to advection and/or natural and predation mortality of *Calanus* spp. by abundant planktivorous predators would explain the much lower biomass observed in fall relative to spring during some years.

The annual abundances of key copepod species in the three regions are shown in Figures 28, 29, and 30. The annual mean abundance of *C. finmarchicus* was similar in 2011 and 2012 in the wGSL and eGSL but greater in 2012 than in 2011 in the sGSL (Fig. 28). When a longer period is considered, *C. finmarchicus* abundances in 2011 and 2012 were lower than during the period of high abundance observed in the mid-2000s. For *C. hyperboreus*, the mean 2012 abundance was greater than in 2011 across the GSL and higher than most years in the wGSL and sGSL (Fig. 29). Total abundance of this species appeared to drive the interannual pattern in zooplankton biomass, although the increase in zooplankton biomass from 2011 to 2012 appeared smaller than what would have been expected based on *Calanus* species abundance (Fig. 28, 29). The mean annual *Pseudocalanus* spp. abundance was lower in 2012 relative to 2011 in all regions, and the abundances for both years were lower than the 2010 maximum, which was the culminating point of a period of increasing abundance that started in 2005 (Fig. 30).

Copepod phenology

We present a detailed figure showing the seasonal cycle of the relative proportions of *C. finmarchicus* copepodite stages at Rimouski station from 1994 to 2012 in order to provide—for the first time—an assessment of potential changes in the phenology of zooplankton in the GSL (Fig. 31). We used proportions to minimize any distortion caused by large interannual variations in absolute abundance (see Fig. 20a, 32). The comprehensive examination of this data set revealed notable changes in the timing of the development of this key copepod species. For example, the period of maximum contribution of stages CI–III (equivalent to their abundance maximum) shifted from mid to late July during the 1994–2000 period to predominantly mid-June to early July in 2006–2012 (Fig. 31). This trend toward earlier development in summer stages was also observed in CIV and CV stages (Fig. 31). The occurrence of a second generation of CI–III and CIV in late summer and/or late fall was also more common from 2003 to 2012 than during previous years (see light blue to orange areas from August to October in Fig. 31). Long-term changes in the timing of maximum occurrence were also observed for stage CVI (both sexes), with an earlier timing from 2008–2012 relative to 1994–2005 (Fig. 31). These changes in the phenology of *C. finmarchicus* mirrored those in the stage structure of the overwintering population of *C. hyperboreus* (data not shown), suggesting that variations in the physical, chemical, and biological environmental conditions influence the intrinsic dynamics of these key copepod species, not only their overall abundance and productivity.

Scorecards

A synthesis of basic AZMP zooplankton indices (abundances of *C. finmarchicus*, *Pseudocalanus* spp., total copepods, non-copepods) was performed using annual standardized

abundance anomalies and is presented as a scorecard (Fig. 32). In general, these annual indices were relatively coherent through the time series among the fixed stations, sections, and large regions. After two years of strong negative abundance anomalies in 2009 and 2010, *C. finmarchicus* remained below normal in all regions (in the sGSL in particular) in 2011 but increased to near-normal values in 2012. The smaller *Pseudocalanus* spp. showed the opposite pattern, with a high positive abundance anomaly in 2011 in all regions following two years of abundances well above the normal in 2009–2010 and a decrease to near-normal abundance in 2012. Total copepod abundance was generally close to the long-term normal in 2011 but showed a negative anomaly in 2012. Finally, a strong positive anomaly in non-copepod abundance (by up to four standard deviations) in the eGSL was observed in 2011; it decreased markedly in 2012 to near-normal values in the wGSL and eGSL while remaining above normal in the sGSL. This index is strongly influenced by meroplankton taxa (larval stages of various benthic invertebrates) and larval euphausid stages (eggs, nauplii).

The annual standardized abundance anomalies for a new set of zooplankton indices are presented in Figure 33. Again, these annual indices were relatively coherent among the fixed stations, sections, and large regions over the time series. *C. hyperboreus* abundance was well above the long-term normal in 2012 after the near- to below-normal values in 2011; this coincided with the *C. finmarchicus* increase between 2011 and 2012 (Fig. 32) and resulted in a larger-than-normal abundance of large calanoids in 2012 (Fig. 33). This positive anomaly in large-bodied copepods has not been observed in the GSL since 2008. Overall, small calanoid abundances remained near or above normal in 2011 and 2012, indicating that the decrease in *Pseudocalanus* spp. in 2012 (Fig. 32) was compensated by an increase in the abundance of other taxa. Most notably, the warm-water species *Centropages* spp. and *Paracalanus* spp. showed their highest abundances of the time series (strong positive anomaly) in 2011 and 2012 (Fig. 33). Considering the GSL as a whole, the small cyclopoids (dominated by *Oithona* spp.) were below or near normal in 2011 and 2012, respectively, which could have contributed to the negative total copepod anomaly observed in 2012 (Fig. 32, 33). Finally, the abundance of cold/arctic copepod species (*C. glacialis*, *M. longa*) was well above normal in 2011 but showed a marked decrease to near-normal abundance in 2012 (Fig. 33).

DISCUSSION

In 2011 and 2012, a set of physical indices, including surface and cold intermediate layer temperature as well as ice season duration, indicated temperature conditions well above the normal; this trend had begun in 2010 (Galbraith et al. 2013). In 2012, this composite index showed its highest value since 1980 and the second highest since 1971; additionally, deep-water temperature in the GSL sharply increased in 2012 to values seldom observed since the early 1980s (Galbraith et al. 2013). Therefore, the present document reports on chemical and biological conditions in the GSL in the context of a strong warming event that began in 2008, which was the last year with a below-average surface temperature index in the GSL (Galbraith et al. 2013).

Winter maximum nutrient inventories in 2011, and to a lesser degree in 2012, were below the 2002–2010 average in many areas of the Estuary and GSL. This trend has been evident since 2008, as revealed by the increased frequency of strong negative anomalies across various GSL subregions. Winter mixing is a critical process to bring nutrient-rich deep water to the surface. In the GSL, this winter convection is in part caused by buoyancy loss (cooling and reduced runoff), brine rejection associated with sea-ice formation, and wind-driven mixing prior to ice formation (Galbraith 2006). In 2011 and 2012, the higher-than-normal average water temperature/stratification and the lower-than-normal ice formation (Galbraith et al. 2013) may have reduced the thickness of the vertical mixing, which limited the supply of start-up nutrients

for primary producers (Plourde and Therriault 2004) and therefore reduced total annual primary production. In addition to vertical mixing, a reduction in upwelling at the head of Laurentian Channel and/or of transport of nutrients via the Gaspé Current may also have contributed to the below-normal winter nutrient inventories for the estuarine portion and freshwater-influenced subregions of the GSL, notably in 2011. In contrast to expectations, the remote sensing of ocean colour data nevertheless revealed that the magnitude of the spring phytoplankton blooms in many areas of the GSL was above normal, especially in 2012.

Changes in stratification can have either positive or negative effects on primary production depending on water column conditions (Ferland et al. 2011). Changes in the ice cover can also influence primary production by its influence on the light conditions in the water column (Le Fouest et al. 2005). The low ice volume and the higher-than-normal average stratification (Galbraith et al. 2013) may have contributed to the markedly early but sometimes intense spring blooms in recent years. On the other hand, the persistence of strong stratification during spring, summer, and fall in 2011 and especially in 2012 (Galbraith et al. 2013) may have reduced phytoplankton production by inhibiting nutrient mixing into surface waters, as is suggested by the strong prevalence of below-normal chlorophyll and nitrate levels observed since 2010 during the post spring-bloom period.

In the lower St. Lawrence Estuary, the situation is somewhat different: the timing of the bloom was relatively close to the normal in 2011 and 2012. In this region, the spring bloom timing is recognized to be largely influenced by both runoff intensity and freshwater-associated turbidity (Levasseur et al. 1984, Therriault and Levasseur 1985; Zakardjian et al. 2000, Le Fouest et al. 2010, Mei et al. 2010). The spring bloom typically starts just after the spring-summer runoff peak. The shorter residence times and weak light conditions during higher freshwater runoff periods are two possible explanations for the delay in phytoplankton growth in this region in early summer compared to early spring in the GSL.

A shift to a smaller-sized phytoplankton community has also been observed in recent years at the Rimouski (since 2004) and Shediac Valley (since 2009) fixed stations, although this phenomenon was less notable in 2011–2012, especially in the St. Lawrence Estuary. In addition, the relative abundance of dinoflagellates has tended to be predominantly higher than normal in recent years. Flagellates and dinoflagellates are typical of a community dominated by recycled production than new production; this situation is consistent with higher nutrient limitation in the post-bloom period (Ferland et al. 2011). Warmer temperatures are also associated with a shift toward greater flagellate and dinoflagellate predominance (Levasseur et al. 1984, Li and Harrison 2008), with potential consequences on copepod recruitment and zooplankton composition as well as on the flow of energy in marine food webs.

In 2012, zooplankton biomass increased relative to 2011 but much less than expected from the observed increase to near normal (*C. finmarchicus*) and record high (*C. hyperboreus*) abundances of *Calanus* species (Fig.16, 32, 33). The smaller body size of *C. finmarchicus* and changes in the relative stage proportion toward a dominance of CIV (smaller than CV and CVI) in *C. hyperboreus* (Fig. 22) would explain why the increase in zooplankton biomass from 2011 and 2012 was of smaller amplitude than the increase in *Calanus* species abundance (see below).

Finding abundances of these arctic and subarctic large-bodied species to be near or well above normal during the near-record high surface temperature in 2012 appears counterintuitive. However, the active growth phase of *C. hyperboreus* occurs from April to June in the GSL, and this species migrates to its deep diapause habitat (>200 m) in early July (Fig. 17c) (Plourde et al. 2003). *C. finmarchicus* mainly reproduces and grows in spring and early summer, and enters diapause in late July to early August in the wGSL (Fig. 17b) (Plourde et al. 2001, Johnson et al.

008). *C. finmarchicus* has also been observed to actively avoid warm and stratified surface aters in order to exploit subsurface habitats (refuges) where it can reproduce and develop Williams 1985, Jónasdóttir and Koski 2011). In 2012, for example, temperatures > 12–13°C, hich are potentially detrimental for the physiology of *C. finmarchicus* late stages, were stricted to the upper 20 m, a depth below which subsurface phytoplankton blooms are ommonly observed in the region (Helaouët and Beaugrand 2007, Møller et al. 2012, Galbraith al. 2013). These characteristics suggest that these species may avoid or adapt their life cycle rategy to minimize the potential negative impacts of warm conditions like those observed in te summer and fall 2012. However, the long-term effect of such warm conditions on the overall uccess of these species has yet to be determined.

ven though the overall success (abundance) of *Calanus* species was normal or above normal 2012 despite record-high water temperatures, the warm surface conditions affected various spects of their population dynamics (ontogeny). The greater relative proportion of CIV in verwintering *C. hyperboreus* in fall 2011 and 2012 relative to the long-term climatology uggests a change in the development rate and the overall life cycle strategy of this species Plourde et al. 2003). Changes toward an earlier period of high CVI abundance and recruitment early stages CI–III as well as evidence for a more predominant second generation in fall were lso observed in *C. finmarchicus* over the last decade (Fig. 31). Moreover, *C. finmarchicus* CV fall 2012 were smaller than usual in the GSL while the body size of CVIf captured at Rimouski tation has shown a long-term negative trend since the cold period in the mid-1990s (Plourde et . 2013). These modifications to the phenology are evidence of the direct effects of changes in e physical (ice dynamics, surface temperature) and biological (phytoplankton bloom timing, uration, and amplitude) environment that have occurred in the region over the last few years Plourde et al. 2013). In the long term, changes in the body size of *Calanus* species could affect e fecundity potential and overwintering capacity of CVIf, which are likely mediated by energy torage (Plourde et al. 2001, 2003, Maps et al. 2010). Overall, changes in phenology and body ze detected in *Calanus* species were relatively strong; these could be useful indices to nplement in AZMP to measure the effects of climate change on the dynamics of lower trophic vels in the ecosystem.

he small calanoids showed marked changes in 2011 and 2012 relative to previous years that ould be associated with concomitant changes in environmental conditions (Fig. 32, 33). Most of ese small species appear to thrive in summer and fall following the peak in surface-dwelling *alanus* species abundance in spring and early summer, suggesting that abnormally high water mperatures in late summer and fall 2012 (and in 2011 to a lesser extent) might have fluenced their success in the region (Plourde et al. 2002). The abundance of *Pseudocalanus* op., a species complex observed from Georges Bank to the Canadian Arctic and widely stributed in the GSL, decreased to near normal from 2011 to 2012, while warm-water species uch as *Paracalanus* spp. and *Centropages* spp. (*C. typicus* in particular) showed record-high undances in 2011 and 2012. High abundances of warm-water species (> 6 standard eviations above normal) were observed in the shallow sGSL and the eGSL in 2012 (Fig. 33); oth of these regions were much warmer than the wGSL in summer and fall and were directly ffected by water originating from the adjacent continental shelf (Galbraith et al. 2013). The creased abundance of warm-water species in 2011 and 2012 was associated with the marked arming of the GSL initiated in 2010 (Galbraith et al. 2013).

he abundances of cold/arctic species (*C. glacialis*, *M. longa*) were well above normal in 2011 nd remained near normal in the very warm conditions observed in 2012. Intuitively, one would ave expected a lower abundance of cold/arctic species during these warm years, which were haracterized by a strong positive anomaly in warm-water species. This apparent discrepancy ould be attributed to the fact that AZMP hydrographic sections often cross distinct waters

ses of different origins. For example, the proportion of *M. longa* / (*M. longa* + *M. lucens)* and *lacialis* / (*C. finmarchicus* + *C. glacialis)* were greater on the northwest half (Québec side) on the southeast half (Newfoundland side) of the TBB section in fall 2012 (not shown). le the Newfoundland end of TBB is under the influence of water entering the eGSL through ot Strait, waters along the northern Québec coast principally originate from the inner rador Shelf (Galbraith et al. 2013). A greater ratio of cold/arctic species in this area could lt either from their transport through the Strait of Belle Isle from the inner Labrador Shelf, colder local environmental conditions more suitable for these cold/arctic species, or both. ater abundances of warm-water species such as *Centropages*, *Paracalanus*, and—for the time—*Clausocalanus* were also observed along the Newfoundland coast in fall 2012 on the and TDC sections. These observations reinforce the transitional status of the GSL, which is ted between the colder "upstream" Labrador/Newfoundland shelf and the more temperate vnstream" Scotian Shelf. Finally, identification of the morphologically similar species *C. archicus* / *C. glacialis* (and potentially *M. lucens* / M. *longa*) using constant body size criteria d be problematic under the varying environmental conditions prevailing at the scale of the MP, with a larger impact being on the rarer species (*C. glacialis* in the case of the GSL) ent et al. 2011, Gabrielsen et al. 2012). Therefore, these results should be considered with until the problem is better quantified.

SUMMARY

This document reports on the chemical and biological (plankton) conditions in the GSL in 2011 and 2012 in the context of a strong warming event initiated in 2008. Data from these two years are compared to time-series observations starting in 1999.

One of the most prominent events in 2011–2012 is that winter, spring, and fall surface nitrate inventories were below normal in many regions of the Gulf, probably due to the persistent higher-than-normal average water temperature/stratification and the below-normal ice conditions.

A shift to earlier timing of the spring bloom is clearly evident in the increased frequency of strong negative anomalies since 2010 across all subregions of the GSL. In addition, chlorophyll levels during summer and fall have tended to be below normal since 2010.

There is evidence of a shift to a smaller phytoplankton community and higher relative abundance of dinoflagellates at the Rimouski and Shediac Valley stations that began in 2004.

The seasonal zooplankton biomass climatologies were similar at the two deep fixed stations (Rimouski, Anticosti Gyre) and showed fall maxima associated with increased abundances of *Calanus* spp., especially in the deep water layer. Biomass climatologies were also similar at the shallow stations (Gaspé Current, Shediac), again largely due to surface-dwelling *Calanus* spp. abundances. Biomass in 2012 increased relative to 2011.

In 2011 and 2012, fixed station abundances of *C. finmarchicus* were below and those of *C. hyperboreus* near or above the 1999–2010 long-term averages. The abundance of small calanoids (*Pseudocalanus* spp.) was strikingly different between 2011 and 2012 at Rimouski station: greater in late 2011 while normal or below normal in 2012.

There is evidence of ontogenetic and phenological changes in *Calanus* species that appear to be the direct effects of the warmer environmental conditions experienced by the region over the last few years. Variations in the physical, chemical, and biological environmental conditions influence the intrinsic dynamics of these key copepod species,

not only their overall abundance and productivity. These changes could prove to be useful indices to measure the effects of climate change on lower trophic levels of the ecosystem.

Total zooplankton biomass was higher in 2012 than in 2011, but lower than expected based on *Calanus* species abundances alone, likely because the stage CIV proportion (relative to older/larger stages) of the large-bodied *C. hyperboreus* was higher than usual.

Total zooplankton biomass in the sGSL in spring showed greater interannual variability than in other GSL regions and was much higher than in fall for several years. This pattern was not observed in the wGSL or eGSL, which may be due to advection and/or mortality (natural or predation).

All standard zooplankton abundance indices were relatively coherent through the time series among fixed stations, sections, and large subregions. *C. finmarchicus* and total copepod abundances were at or somewhat below normal in 2011–2012 while *Pseudocalanus* spp. and non-copepod abundance indices were strongly positive.

High abundances of arctic and subarctic large-bodied species occurred simultaneously with the near-record high surface temperature in 2012, suggesting that these species avoid or adapt their life cycle strategy to minimize potential negative effects of warm conditions; the long-term effects of such high temperatures remain unknown.

There was an increased abundance of warm-water species (*Paracalanus* spp. and *Centropages* spp.) in 2011–2012 associated with marked warming that started in 2010.

High abundances of cold/arctic species concomitant with those of warm-water species likely reflect the complex hydrography of the GSL system and point out its position as a transitional zone between the "upstream" Labrador/Newfoundland shelf and the "downstream" Scotian Shelf.

ACKNOWLEDGEMENTS

ank Jean-Yves Couture and Sylvie Lessard as well as Isabelle St-Pierre and Caroline ır for preparation and standardization of the phytoplankton and zooplankton data, ctively. The data used in this report would not be available without the work of François euve and his team (Sylvain Chartrand, Rémi Desmarais, Marie-Lynn Dubé, Yves Gagnon, McLaughlin, Roger Pigeon, Daniel Thibault, and the late Sylvain Cantin) for organizing and ng out AZMP cruises. Marie-France Beaulieu performed all zooplankton sample analyses. ank Jeff Spry for providing data from the Shediac Valley fixed station and BIO's remote ng unit for the composite satellite images.

REFERENCES

man, D., and B. Petrie. 2003. Nitrate, silicate and phosphate atlas for the Gulf of St. Lawrence. Can. Tech. Rep. Hydrogr Ocean Sci. 231: xi+152 pp.

2013. Oceanographic conditions in the Atlantic zone in 2012. DFO Can. Sci. Advis. Sec. Sci. Advis. Rep. 2013/057.

nd, J., M. Gosselin, and M. Starr. 2011. Environmental control of summer primary production in the Hudson Bay system: The role of stratification. J. Mar. Syst. 88(3): 385–400.

n, T. M., B. Merkel, J. E. Soreide, E. Johansson-Karlsson, A. Bailey, D. Vogedes, H. ard, O. Varpe, and J. Berge. 2012. Potential misidentifications of two climate indicator cies of the marine arctic ecosystem: *Calanus glacialis* and *C. finmarchicus*. Polar Biol. 1): 1621–1628.

P. S. 2006. Winter water masses in the Gulf of St. Lawrence. J. Geophys. Res., 111, 022, doi:10.1029/2005JC003159.

P. S., R. Desmarais, R. Pigeon, and S. Cantin. 2006. Ten years of monitoring winter er masses in the Gulf of St. Lawrence by helicopter. AZMP Bulletin PMZA 5: 32–35 ://www.meds-sdmm.dfo-mpo.gc.ca/isdm-gdsi/azmp-pmza/docs/bulletin_5_08.pdf).

P. S., J. Chassé, D. Gilbert, P. Larouche, D. Brickman, B. Pettigrew, L. Devine, A. selin, R. G. Pettipas, and C. Lafleur, 2012. Physical oceanographic conditions in the of St. Lawrence in 2011. DFO Can. Sci. Advis. Sec. Res. Doc. 2012/023. iii + 85 pp.

P. S., J. Chassé, P. Larouche, D. Gilbert, D. Brickman, B. Pettigrew, L. Devine, and afleur. 2013. Physical oceanographic conditions in the Gulf of St. Lawrence in 2012.) Can. Sci. Advis. Sec. Res. Doc. 2013/026: v + 90 pp.

P., and G. Beaugrand. 2007. Macroecology of *Calanus finmarchicus* and *C. olandicus* in the North Atlantic Ocean and adjacent seas. Mar. Ecol. Prog. Ser. 345: –165.

C. L., A. W. Leising, J. A. Runge, E. J. H. Head, P. Pepin, S. Plourde, and E. G. oin. 2008. Characteristics of *Calanus finmarchicus* dormancy patterns in the Northwest ntic. ICES J. Mar. Sci. 65(3): 339–350.

ir, S. H., and M. Koski. 2011. Biological processes in the North Sea: comparison of *anus helgolandicus* and *Calanus finmarchicus* vertical distribution and production. J. kton Res. 33: 85–103.

ky, V. G., and G. L. Bugden. 1991. The physical oceanography of the Gulf of St. rence: a review with emphasis on the synoptic variability of the motion. In: J.-C. rriault (ed.) The Gulf of St. Lawrence: small ocean or big estuary? Can. Spec. Publ. . Aquat. Sci. 113: 57–90.

, V., B. Zakardjian, F. Saucier, and M. Starr. 2005. Seasonal versus synoptic ability in planktonic production in a high-latitude marginal sea: the Gulf of St. Lawrence nada). J. Geophys. Res. 110, C09012, doi 10.1029/2004JC002423.

, V., B. Zakardjian, and F. J. Saucier. 2010. Plankton ecosystem response to nwater-associated bulk turbidity in the subarctic Gulf of St. Lawrence (Canada): A delling study. J. Mar. Syst. 81(1–2): 75–85.

r, M., J.-C. Therriault, and L. Legendre 1984. Hierarchical control of phytoplankton cession by physical factors. Mar. Ecol. Prog. Ser. 19: 211–222.

W., and W. G. Harrison. 2008. Propagation of an atmospheric climate signal to oplankton in a small marine basin. Limnol. Oceanogr. 53(5): 1734–1745.

S. Plourde, and B. Zakardjian. 2010. The control of dormancy by lipid metabolism in *anus finmarchicus*: a population model test. Mar. Ecol. Prog. Ser. 403:165–180.

F., M. Maar, S. H. Jónasdóttir, T. G. Nielsen, and K. Tönnesson. 2012. The effect of nges in temperature and food on the development of *Calanus finmarchicus* and *anus helgolandicus* populations. Limnol. Oceanogr. 57: 211–220.

F. Saucier, V. Le Fouest, B. Zakardjian, S. Sennville, H. Huixiang Xie, and M. Starr. Modeling the timing of spring phytoplankton bloom and biological production of the of St. Lawrence (Canada): Effects of colored dissolved organic matter and erature. Cont. Shelf Res. 30: 2027–2042.

R., G. Harrison, K. Pauley, A. Gagné, G. Maillet, and P. Strain. 2002. Atlantic Zonal oring Program sampling protocol. Can. Tech. Rep. Hydrogr. Ocean Sci. 223, iv + 23

S. Plourde, and J. Turgeon. 2011. Overlapping size ranges of *Calanus* spp. off the dian Arctic and Atlantic Coasts: impact on species' abundances. J. Plankton Res. 33: -1665, doi:10.1093/plankt/fbr072.

S. Plourde, C. DiBacco, G. Winkler, and P. Sirois. 2014. Tracing the origins of *us* sp. in the Saguenay-St. Lawrence Marine Park (Québec, Canada) using $\delta^{13}C$ as ker. Mar. Ecol. Prog. Ser., 499: 89–102, doi: 10.3354/meps10651.

and J.-C. Therriault. 2004. Climate variability and vertical advection of nitrates in the of St. Lawrence, Canada. Mar. Ecol. Prog. Ser., 279: 33–43.

P. Joly, J. A. Runge, B. Zakardjian, and J. J. Dodson. 2001. Life cycle of *Calanus rchicus* in the lower St. Lawrence Estuary: imprint of circulation and late plankton bloom. Can. J. Fish. Aquat. Sci. 58: 647–658.

J. J. Dodson, J. A. Runge, and J.-C. Therriault. 2002. Spatial and temporal ions in copepod community structure in the lower St. Lawrence Estuary, Canada. Ecol. Prog. Ser. 230: 221–224.

P. Joly, J. A. Runge, J. Dodson, and B. Zakardjian. 2003. Life cycle of *Calanus rboreus* in the lower St. Lawrence Estuary: is it coupled to local environmental tions? Mar. Ecol. Prog. Ser. 255: 219–233.

F. Maps, and P. Joly. 2009. Mortality and survival in early stages control tment in *Calanus finmarchicus*. J. Plankton Res. 31(4): 371–388.

P. Galbraith, V. Lesage, F. Grégoire, H. Bourdage, J.-F. Gosselin, I. McQuinn, and arratt. 2013. Ecosystem perspective on changes and anomalies in the Gulf of St. ence: a context in support of the management of the St. Lawrence beluga whale ation. DFO Can. Sci. Advis. Sec. Res. Doc. 2013/129. v + 30 pp.

., M. Castonguay, Y. de Lafontaine, M. Ringuette, and J. L. Beaulieu. 1999. riation in climate, zooplankton biomass and mackerel recruitment in the southern of St Lawrence. Fish. Oceanogr., 8: 139–149.

.-C., and M. Levasseur. 1985. Control of phytoplankton production in the Lower St. ence Estuary: light and freshwater runoff. Nat. Can.112: 77–96.

.-C., B. Petrie, P. Pépin, J. Gagnon, D. Gregory, J. Helbig, A. Herman, D. Lefaivre, tchell, B. Pelchat, J. Runge, and D. Sameoto. 1998. Proposal for a Northwest ic zonal monitoring program. Can. Tech. Rep. Hydrogr. Ocean Sci., 194: vii + 57 pp.

. 1985. Vertical distribution of *Calanus finmarchicus* and *C. helgolandicus* in relation development of the seasonal thermocline in the Celtic Sea. Mar. Biol. 86: 145–149.

B. A., Y. Gratton, and A. F. Vézina. 2000. Late spring phytoplankton bloom in the r St. Lawrence Estuary: the flushing hypothesis revisited. Mar. Ecol. Prog. Ser. 192: 3.

f AZMP cruises with locations, dates, and sampling activities for 2011 and 2012. The s start with "T" (transect) followed by the French abbreviations for the geographical SL: St. Lawrence Estuary; TSI: Sept-Îles; TASO: southwest Anticosti; TIDM: Îles-de-la-DC: Cabot Strait; TCEN: Gulf centre; TBB: Bonne Bay; wGSL, eGSL, and sGSL denote the ern, and southern subregions of the Gulf of St. Lawrence. See Figure 1 for the map showing ns.

ng			2011				2012			
	Name	Location	Dates	Vessel	Hydro	Net	Dates	Vessel	Hydro	Net
	Rimouski	48°40.0'N/068°35.0'W	13 APR-12 OCT	Beluga I and II	19	19	03 APR-27 NOV	Beluga II	26	26
	Gaspé Current	49°14.5'N/066°12.0'W	07 FEB-23 AUG	Multiple	3	3	20 JUN-30 AUG	Multiple	3	3
	Anticosti Gyre	49°43.0'N/066°15.0'W	07 FEB-27 AUG	Multiple	4	4	29 FEB-20 AUG	Multiple	4	4
	Shediac Valley	47°47.0'N/064°02.0'W	26 MAY-29 NOV	Multiple	7	7	20 APR-02 NOV	Multiple	8	8
					33	33			41	41
	TESL	wGSL	01-11 JUN	Teleost	7	7	02-11 JUN	Teleost	7	7
	TSI	wGSL	01-11 JUN	Teleost	6	6	02-11 JUN	Teleost	6	6
	TASO	wGSL	01-11 JUN	Teleost	5	5	02-11 JUN	Teleost	5	4
	TIDM	sGSL	01-11 JUN	Teleost	10	10	02-11 JUN	Teleost	10	10
	TDC	eGSL	01-11 JUN	Teleost	6	6	02-11 JUN	Teleost	6	6
	TCEN	eGSL	01-11 JUN	Teleost	5	4	02-11 JUN	Teleost	5	5
	TBB	eGSL	01-11 JUN	Teleost	7	7	02-11 JUN	Teleost	7	7
					46	45			46	45
	TESL	wGSL	01-14 NOV	Hudson	7	7	01-14 NOV	Hudson	7	7
	TSI	wGSL	01-14 NOV	Hudson	6	6	01-14 NOV	Hudson	6	6
	TASO	wGSL	01-14 NOV	Hudson	5	5	01-14 NOV	Hudson	5	5
	TIDM	sGSL	01-14 NOV	Hudson	10	10	01-14 NOV	Hudson	10	10
	TDC	eGSL	01-14 NOV	Hudson	6	6	01-14 NOV	Hudson	6	6
	TCEN	eGSL	01-14 NOV	Hudson	5	5	01-14 NOV	Hudson	5	5
	TBB	eGSL	01-14 NOV	Hudson	7	7	01-14 NOV	Hudson	7	7
					46	46			46	46

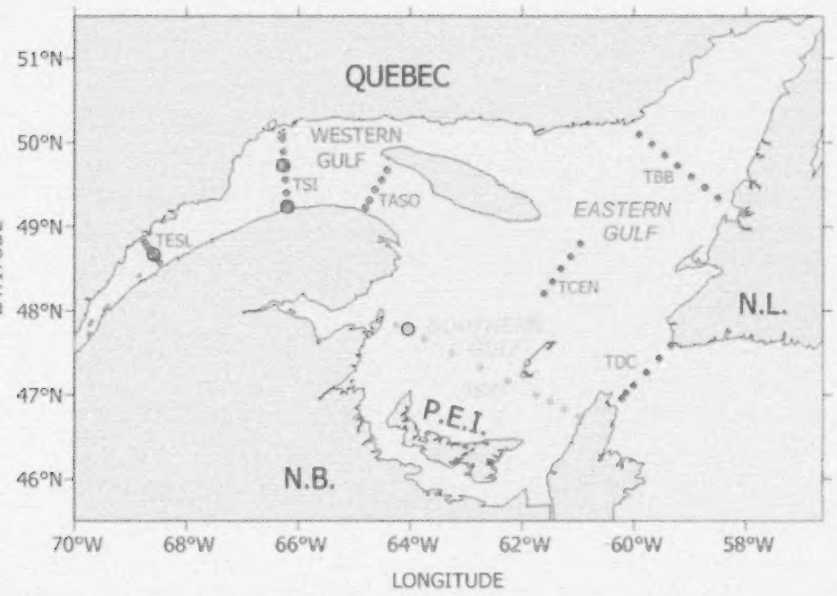

of the Estuary and Gulf of St. Lawrence showing sampling stations on the different sections and at fixed sites (open circles).GSL subregions are the western (red), southern (blue), and) Gulf. The section names start with "T" (transect) followed by the French abbreviations for cal locations: TESL: St. Lawrence Estuary; TSI: Sept-Îles; TASO: southwest Anticosti; la-Madeleine; TDC: Cabot Strait; TCEN: Gulf centre; TBB: Bonne Bay.

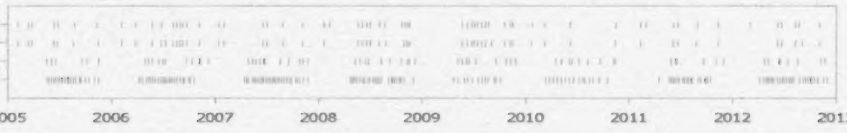

ing frequencies at the fixed stations from 2005 to 2012 to show sampling effort in recent costi Gyre; GC: Gaspé Current; RIKI: Rimouski.

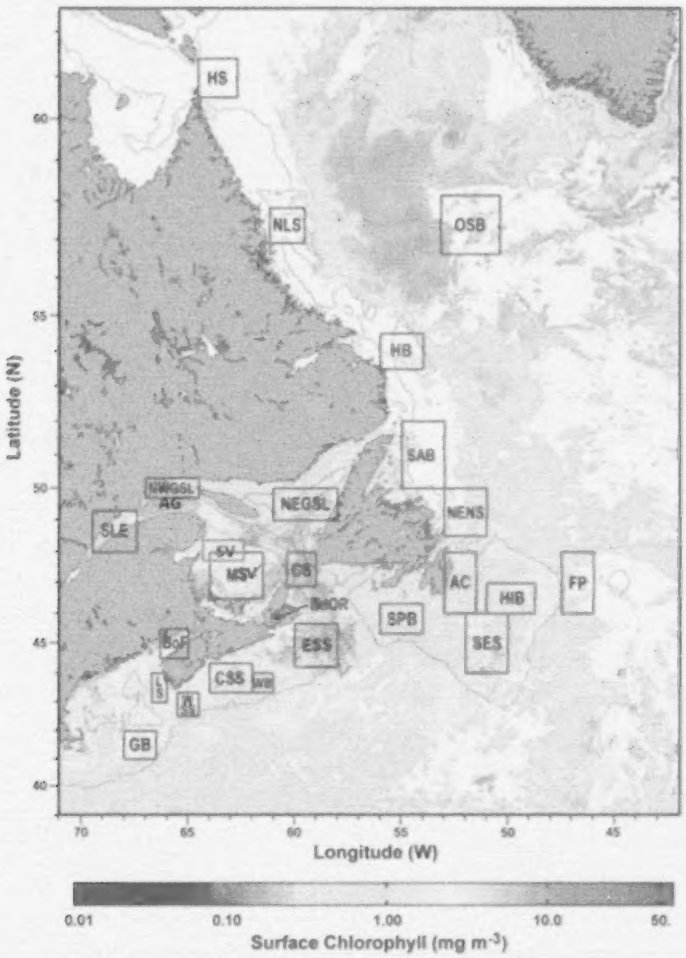

*ical subregions in the Northwest Atlantic identified for spatial/temporal analysis of satellite ta. AC: Avalon Channel; **AG**: **Anticosti Gyre**; BdOR: Bras d'Or; BoF: Bay of Fundy; **CS**: SS: Central Scotian Shelf; ESS: Eastern Scotian Shelf; FP: Flemish Pass; GB: Georges lton Bank; HIB-Hibernia; HS: Hudson Strait; LS: Lurcher Shoal; **MS**: **Magdalen Shallows**; **ast Gulf of St. Lawrence**; NENS: Northeast Newfoundland Shelf; NLS: Northern **NWGSL**: **Northwest Gulf of St. Lawrence**; OSB: Ocean Station Bravo; SAB: St. SES: Southeast Shoal; SLE: St. Lawrence Estuary; SPB: St. Pierre Bank; **SV**: **Shediac** stern Bank; WSS: Western Scotian Shelf. Only data from Gulf of St. Lawrence subregions d) are presented in this report. (The figure is a SeaWiFS composite image showing m 1–15 April 1998.)*

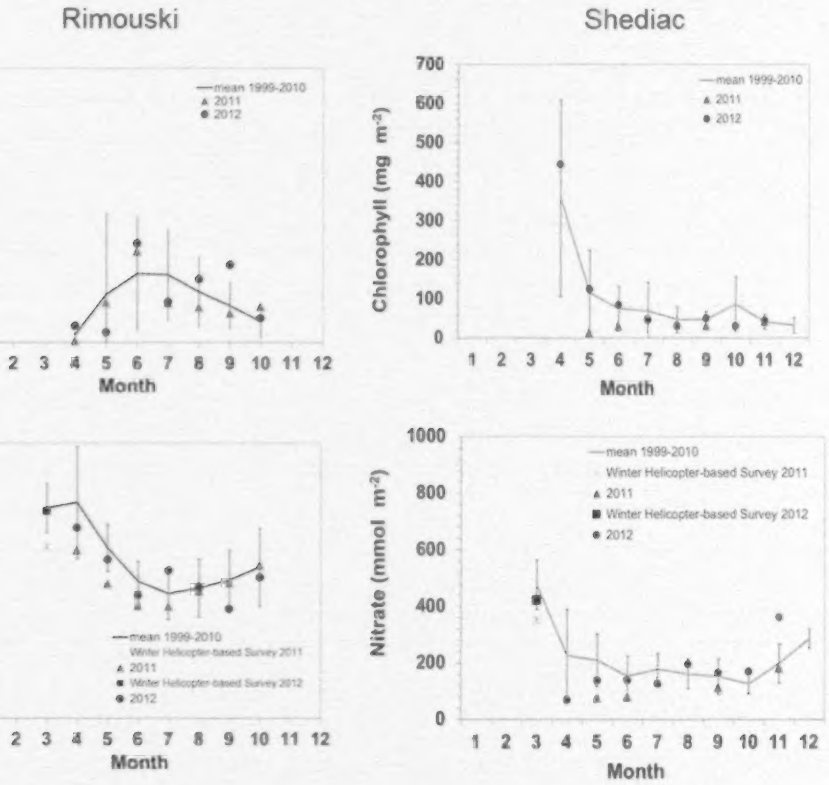

ison of 2011 (triangles) and 2012 (circles) chlorophyll (top panels) and nitrate (bottom s with mean conditions from 1999–2010 (solid line) at the Rimouski and Shediac Valley tical lines are 95% confidence intervals of the monthly mean.Early winter nitrate values h helicopter survey (samples from 2 m). Integrated values were calculated using the 2 ssuming that the nitrate concentrations are homogeneous in the winter mixed layer at ar).

Figure (diato ratios

Station Rimouski

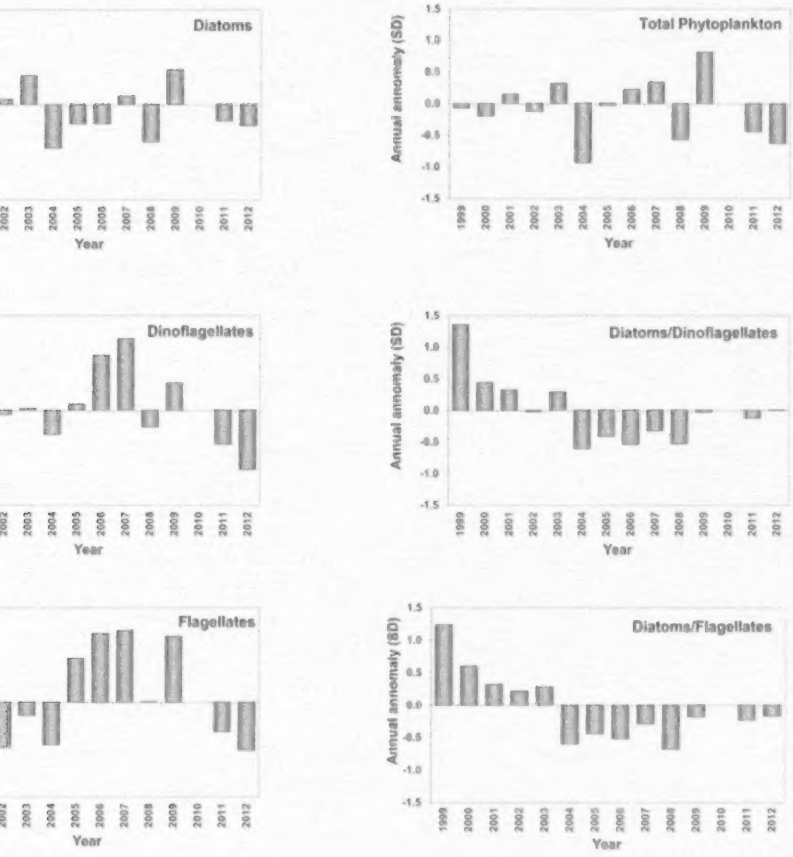

s of microplankton abundance anomalies for total phytoplankton and by group ates, flagellates, ciliates), and for the diatom/dinoflagellate and diatom/dinoflagellate tation, 1999–2012.

Figure 6
2012.

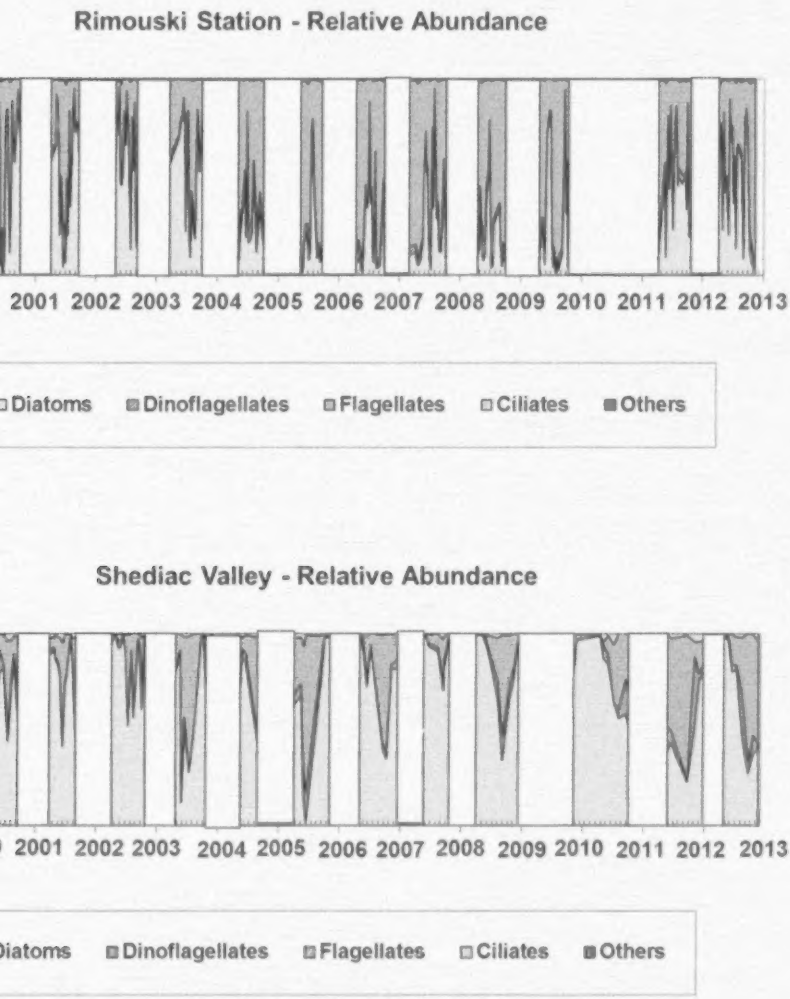

ommunity composition at Rimouski and Shediac Valley fixed stations, 1999–

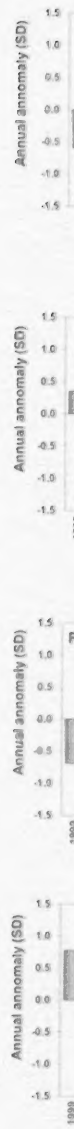

Figure 7. Tim
(diatoms, din
ratios at Shed

Station Shediac

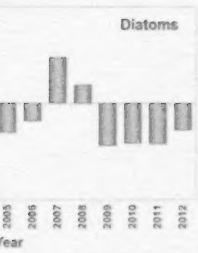

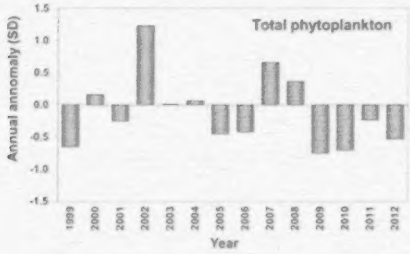

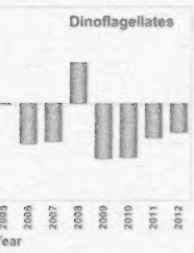

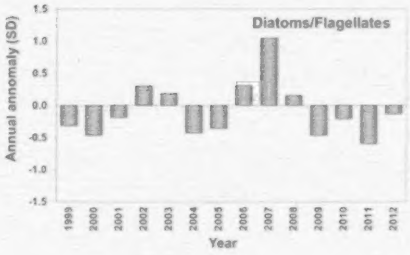

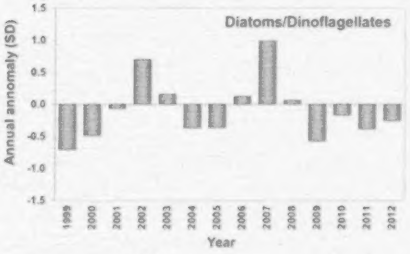

croplankton abundance anomalies for total phytoplankton and by group agellates, ciliates), and for the diatom/dinoflagellate and diatom/dinoflagellate tion, 1999–2012.

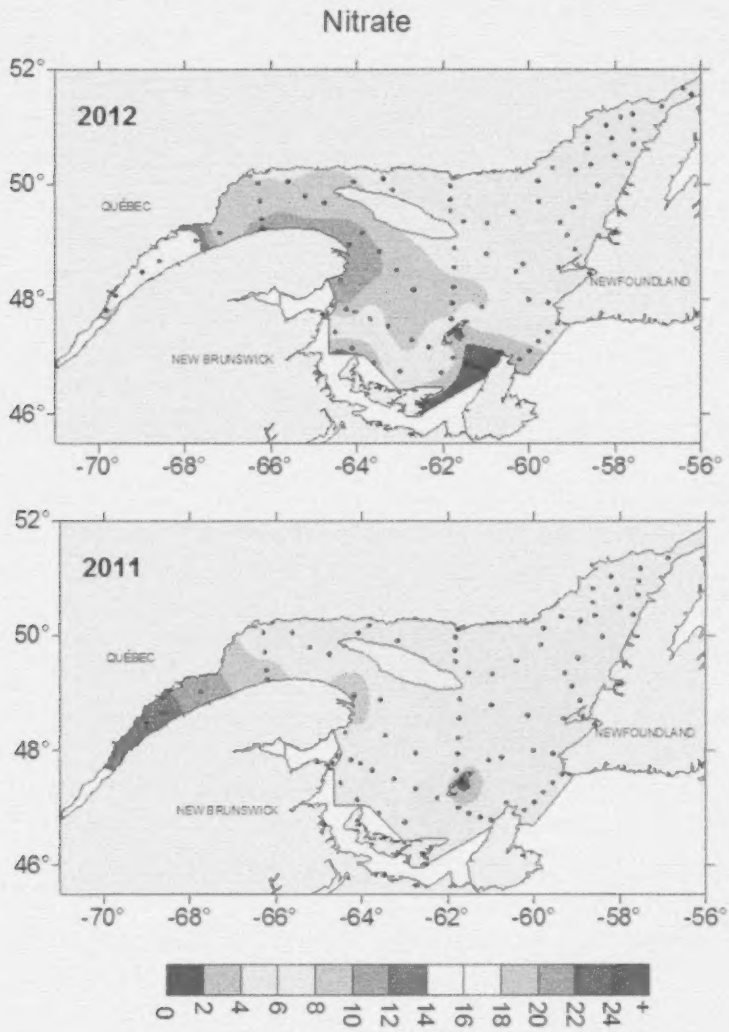

Figure 8. Concentrations of nitrate (mmol m^{-3}) at 2 m collected in the Estuary and Gulf of St. Lawrence during the helicopter survey in late winter (mid-March) 2011 and 2012. Dots indicate sampling locations.

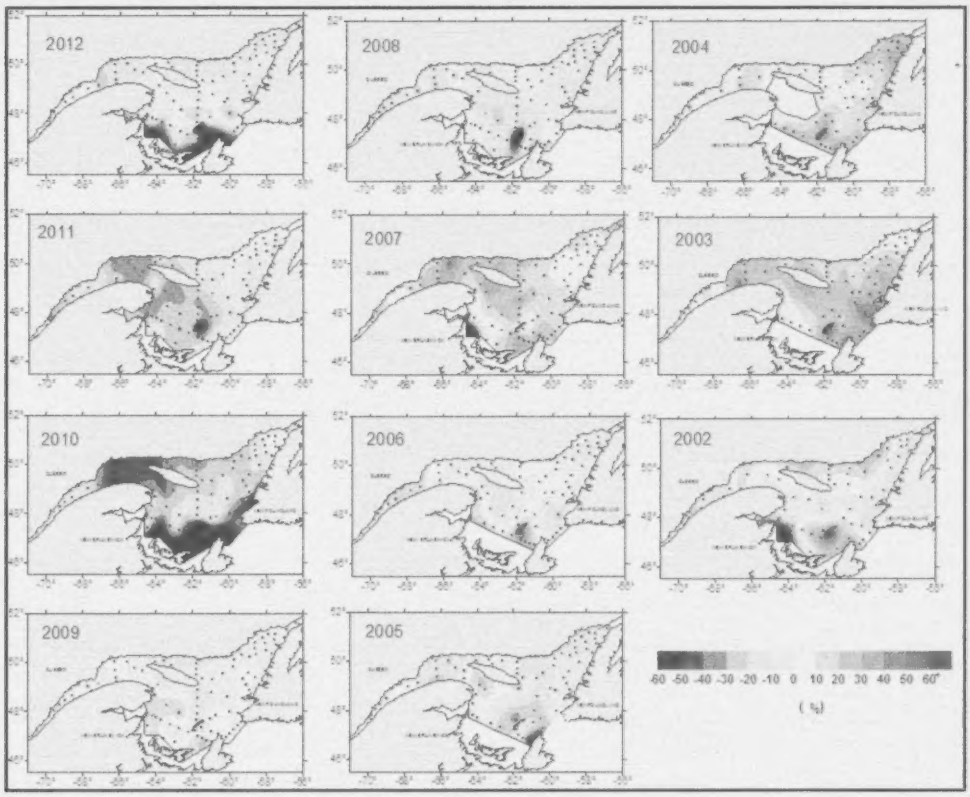

Figure 9. Percentage of change in the late winter (mid-March) nitrate concentrations at 2 m from samples collected during the helicopter survey from 2002 to 2012 relative to the 2001–2010 average. Dots indicate sampling locations.

Index	Transect	1999	2000	2001	2002	2003	2004	2005	2006	2007	2008	2009	2010	2011	2012	Mean	SD
Winter nitrate inventories	TESL			-0.3	-0.6	0.9	0.6		1.5	0.7	-1.5	0.2	-1.5	-1.7	-0.2	770.1	85.5
(0-50m)	TSI			-0.1	0.4	1.2	0.5	-0.8	0.0	1.3	-0.7	0.3	-2.1	-1.2	-0.4	527.7	125.1
(mmol m^{-2})	TASO			-0.2	0.0	1.2	-0.1	0.1	0.3	1.0	-0.1	0.2	-2.5	-1.8	-0.4	521.7	88.6
	TCEN			-0.6	-0.3	1.9	0.8	-0.9	-0.1	1.3	-0.6	-0.6	-0.9	-1.5	0.3	344.3	51.1
	TIDM			0.0	0.4	0.6	0.9	-0.5	0.8	0.5	-0.8	0.4	-2.4	-0.9	-1.3	383.6	98.6
	TBB			-0.3	0.3	1.7	0.9	-0.7	-0.2	0.5	-0.7	0.0	-1.7	-0.5	-0.6	299.0	38.3
	TDC			0.4	0.2	1.3	0.6	-1.0	-0.4	0.7	0.2	0.0	-2.2	-0.4	-1.0	292.5	80.3
Spring nitrate inventories	TESL			0.0	1.7	-0.2	0.4		1.3	-0.8	0.0	-0.9	-1.4	-0.6	0.2	436.8	92.3
(0-50m)	TSI	-1.2	-0.1	1.0	1.4	1.2	-0.7	-0.6	0.0	-0.9	1.5	-0.6	-1.0	-1.0	-0.7	202.6	45.7
(mmol m^{-2})	TASO	-1.5	-0.6	-0.2	1.2	1.1	0.5	-0.7	-0.8	0.8	0.6	0.2	-1.2	-1.0	-1.3	185.6	59.0
	TCEN						-1.5	0.0	1.0	0.0	1.3	0.2	-0.9	-0.9	-1.6	68.2	19.7
	TIDM	-0.8	1.0	-0.8	-0.2	0.3	-0.6	-0.2	1.1	0.0	1.1	0.6	-1.9	-0.5	-1.0	109.4	38.4
	TBB	-0.3	0.3	-0.3	-0.3	-2.5	-1.4	-1.0	-0.1	0.7	0.8	-0.6	-0.3	-1.1	-0.8	62.9	23.9
	TDC	-1.2	1.0	-0.2	-1.5	0.8	-0.1	-1.0	0.0	0.6	2.1	0.0	-0.4	-1.5	-0.7	70.7	21.0
Difference between winter	TESL			-0.3	-1.9	0.9	0.1		0.1	1.2	-1.1	1.0	0.0	-0.8	-0.3	332.0	110.6
and late spring nitrate	TSI			-0.4	-0.1	0.9	0.8	-0.5	0.1	1.6	-1.2	0.5	-1.6	-0.8	-0.1	319.4	126.0
(0-50m)	TASO			0.1	-0.8	0.3	-0.3	0.9	1.4	0.9	-0.5	0.3	-2.1	-1.4	0.8	323.3	65.5
(mmol m^{-2})	TCEN						1.4	-0.7	-0.3	1.4	-0.9	-0.5	-0.4	-0.9	1.0	268.8	54.0
	TIDM			0.3	0.6	0.6	1.3	-0.5	0.2	0.6	-1.4	0.1	-1.9	-0.9	-1.1	274.9	83.8
	TBB			-0.1	0.5	0.4	1.0	-0.1	-0.1	0.1	-1.3	0.4	-1.7	0.2	-0.1	236.1	34.8
	TDC			0.5	0.6	1.2	0.9	-0.8	-0.4	0.6	-0.4	0.0	-2.2	0.0	-0.9	221.3	75.0
Fall nitrate inventories	TESL	2.5	-0.1	0.5	1.1	-0.6	-1.1	0.3	-0.8	-0.8	-0.1	-0.6	-0.3	-0.1	0.7	534.5	115.9
(0-50m)	TSI	1.9	-0.7	1.1	1.2	0.5	-1.3	-1.2	-0.3	-0.7	-0.5	-0.3	0.3	-0.5	1.6	268.0	102.2
(mmol m^{-2})	TASO	1.9	-0.3	0.9	1.2	-1.2	-1.0	-0.6	-0.3	-0.6	0.4	-1.0	0.8	-1.0	1.3	277.8	73.5
	TCEN					-0.1	-0.9	-0.4	-0.3	2.5	0.2	0.5	-1.2	-2.8	1.9	136.1	28.3
	TIDM		1.2	0.6	0.0	-1.2	1.3	0.1	1.3	-0.9	-0.2	-0.9	-1.2	-2.2	-1.3	183.2	36.5
	TBB	0.9	0.3	1.3	0.1	0.8	-1.9	-0.3	-1.6	1.0	-0.4	0.2	-0.5	-0.5	-1.5	125.4	30.5
	TDC	1.4	0.7	-0.2	-2.2	-0.6	-1.3	0.1	-0.1	-0.5	-0.6	-0.2	-0.9	-1.0	-0.5	135.5	45.4
Seasonally adjusted nitrate	TESL	2.6	0.1	0.0	1.0	-0.6	-0.6	0.5	-0.1	-0.9	-0.3	-0.9	-0.9	-0.5	0.2	510.7	120.1
inventories (0-50m)	TSI	1.2	-0.6	1.3	1.6	0.9	-1.3	-1.2	-0.3	-0.9	0.2	-0.5	-0.2	-0.8	1.1	235.3	60.4
(mmol m^{-2})	TASO	0.7	-0.8	0.7	2.2	0.2	-0.7	-1.2	-1.0	0.1	0.8	-0.9	-0.2	-1.8	0.3	231.7	35.8
	TCEN					1.2	-1.4	-0.4	0.1	1.1	0.5	0.2	-1.3	-2.3	-2.1	106.3	22.7
	TIDM	-1.8	1.3	0.0	0.0	-0.4	0.5	0.1	1.7	-0.4	0.6	0.0	-1.5	-1.3	-1.1	141.9	35.7
	TBB	0.4	0.4	0.7	-0.1	1.9	-2.0	-0.7	-1.1	1.0	0.1	-0.1	-0.5	-0.9	-1.4	94.2	23.1
	TDC	1.0	1.4	-0.3	1.6	-0.3	-1.6	-0.4	-0.1	-0.3	0.4	-0.3	-1.3	-2.0	-1.0	103.1	19.4
Seasonally adjusted nitrate	TESL			1.0	1.6	0.2	-1.3		0.5	0.0	-0.5	0.1	-1.5	-1.2	1.0	1335.6	110.5
inventories (50-150m)	TSI	0.0	-1.4	0.7	1.2	0.9	-1.4	-0.9	0.7	-0.2	1.3	-1.1	-0.1	-0.5	1.1	1354.4	143.6
(mmol m^{-2})	TASO	-0.1	-1.5	0.2	1.4	0.9	-1.0	-1.0	1.0	-0.1	1.1	0.4	-1.3	-0.5	2.2	1256.1	100.0
	TCEN						-1.5	-0.3	1.2	0.7	0.3	0.7	-1.1	-0.9	-0.3	1092.6	106.3
	TIDM																
	TBB	-2.6	-0.2	0.0	0.5	1.1	-1.0	-0.1	0.9	0.7	0.1	-0.1	0.7	0.4	0.4	897.5	99.0
	TDC	-1.1	1.9	-1.3	0.0	0.3	-1.1	-0.6	1.9	-0.3	0.5	0.4	-0.1	-0.5	1.6	867.0	86.0

Spring chl concentrations	TESL		0.0	1.0	-0.9	1.7	-0.9	0.0	-1.0	1.1	-0.7	-0.1	-0.2	-0.4	-0.1	153.0	97.5
(0-100m)	TSI	-0.2	-1.4	0.1	2.3	-0.3	1.3	-0.8	0.3	0.2	-0.9	-0.7	0.1	-0.3	0.5	69.5	38.0
(mg Chl m^{-2})	TASO	-0.4	-0.7	-0.7	2.6	-0.4	0.5	0.5	0.4	-0.7	-0.6	-0.6	-0.1	-0.6	-0.1	93.6	67.5
	TCEN						-0.8	-0.6	-0.7	0.6	1.1	0.6	-0.8	-0.8	-0.9	38.3	12.0
	TIDM	-0.2	-1.6	-0.5	2.4	0.3	-0.1	-0.7	0.0	-0.2	-0.4	-0.2	1.2	-0.2	-0.3	34.9	13.8
	TBB	-1.0	0.5	-1.2	1.8	-0.8	1.2	-0.7	-0.8	-0.1	0.8	-0.5	0.4	1.1	-0.4	29.6	10.2
	TDC	2.0	-0.6	0.0	2.1	-0.7	-0.7	-0.7	-0.1	-0.4	-0.5	-0.4	0.1	-0.5	-0.4	47.0	31.8
Fall chl concentrations	TESL	-0.7	-1.6	-0.6	-0.1	1.2	0.2	-0.3	-0.1	0.0	2.4	-0.2	-0.1	-0.4	0.7	23.2	9.0
(0-100m)	TSI	-0.5	-0.9	-0.6	-0.2	0.3	-0.3	0.4	-0.3	-0.2	3.0	-0.5	-0.3	-0.5	-0.3	45.7	33.6
(mg Chl m^{-2})	TASO	-0.6	-1.0	-0.5	-0.2	0.6	-0.5	0.2	-0.1	-0.2	2.9	-0.1	-0.5	-0.3	0.1	45.3	32.1
	TCEN					1.3	-1.4		-0.9	-0.6	0.2	0.3	1.1	-1.5	0.0	41.7	8.3
	TIDM		-1.6	0.6	1.7	0.8	-0.9	-0.9	-0.4	1.2	-0.5	-0.1	0.1	0.5	1.7	38.2	16.5
	TBB	-0.6	-1.4	-0.3	1.4	1.0	2.1	-0.6	-0.7	0.3	-0.6	-0.2	-0.4	1.0	0.8	35.1	10.8
	TDC	-0.9	-1.7	-0.2	1.8	0.4	-0.3	-0.8	0.8	1.1	-0.4	1.3	-0.6	-0.8	-0.7	40.9	11.2
Seasonally adjusted chl	TESL	-1.0	-1.2	1.2	-0.5	1.0	-0.5	-0.9	-0.6	1.3	-0.1	0.2	0.1	-0.1	0.3	70.9	53.5
concentrations (0-100m)	TSI	-0.5	-1.8	-0.4	1.7	-0.1	0.9	-0.4	0.0	0.0	1.5	-1.0	-0.1	-0.6	0.2	57.6	22.3
(mg Chl m^{-2})	TASO	-0.7	-1.1	-0.9	2.6	-0.1	0.3	0.6	0.3	-0.8	0.7	-0.6	-0.4	-0.6	-0.1	69.4	35.9
	TCEN						-1.2	-1.0	-0.9	0.1	1.2	0.5	-0.1	-1.3	-0.6	40.2	9.0
	TIDM	-0.5	-1.5	-0.7	0.9	0.3	-0.2	0.1	-0.2	-0.4	2.5	-0.6	0.4	-0.6	-0.3	36.6	16.2
	TBB	-0.9	-0.5	-0.8	1.7	0.1	2.3	-0.7	-0.9	0.1	0.1	-0.4	0.0	0.0	0.2	32.3	9.2
	TDC	-1.5	-1.1	-0.1	2.4	-0.5	-0.7	-0.9	0.1	-0.1	-0.6	0.1	-0.1	-0.7	-0.6	44.0	17.8

Figure 10. *Normalized annual anomalies (scorecard) for nutrient inventories and chlorophyll levels during the winter, late spring, and fall surveys. Blue colours indicate anomalies below the mean and reds are anomalies above the mean.*

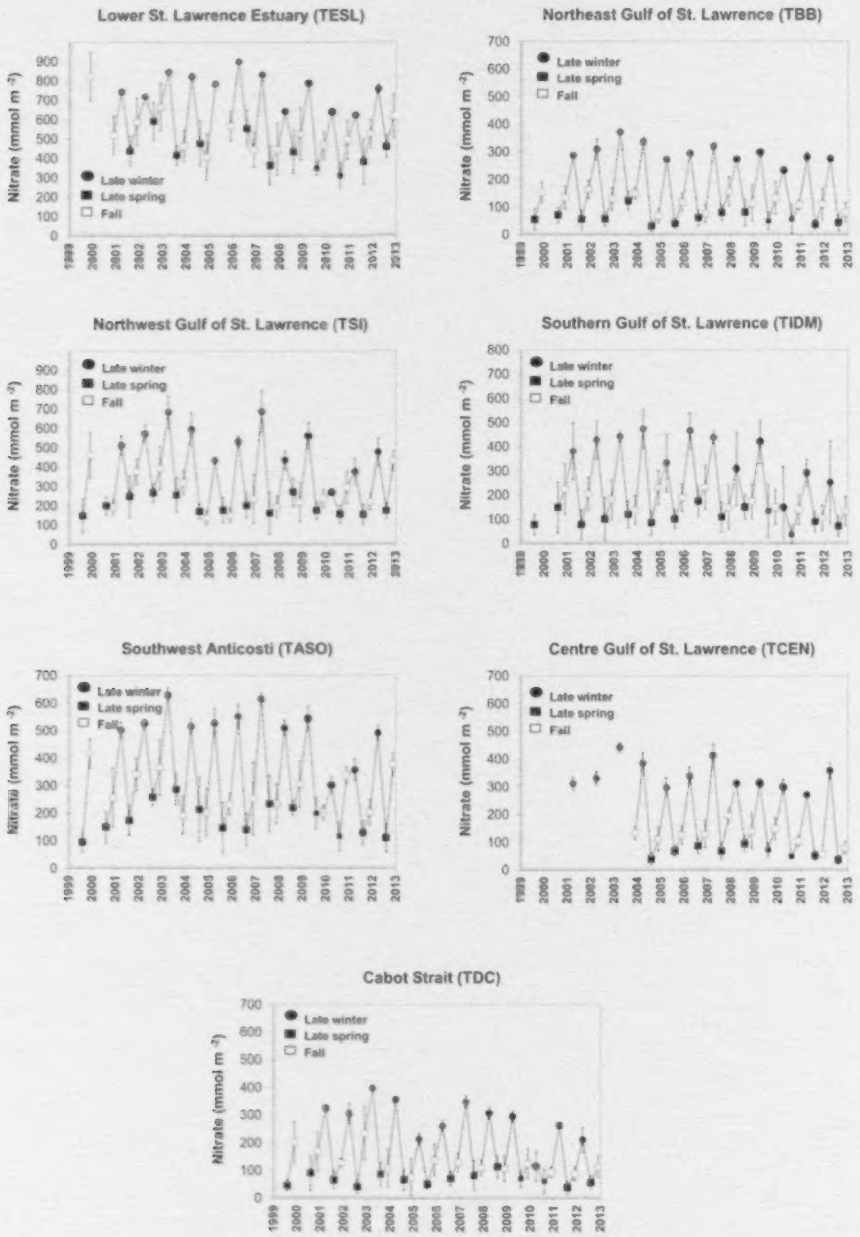

Figure 11. Time series of surface (0–50m) nitrate inventories along the seven AZMP sections from 1999 to 2012. The late winter inventories were calculated using surface concentrations (2 m) × 50 m (assuming that the nitrate concentrations are homogeneous in the winter mixed layer at that time of the year).

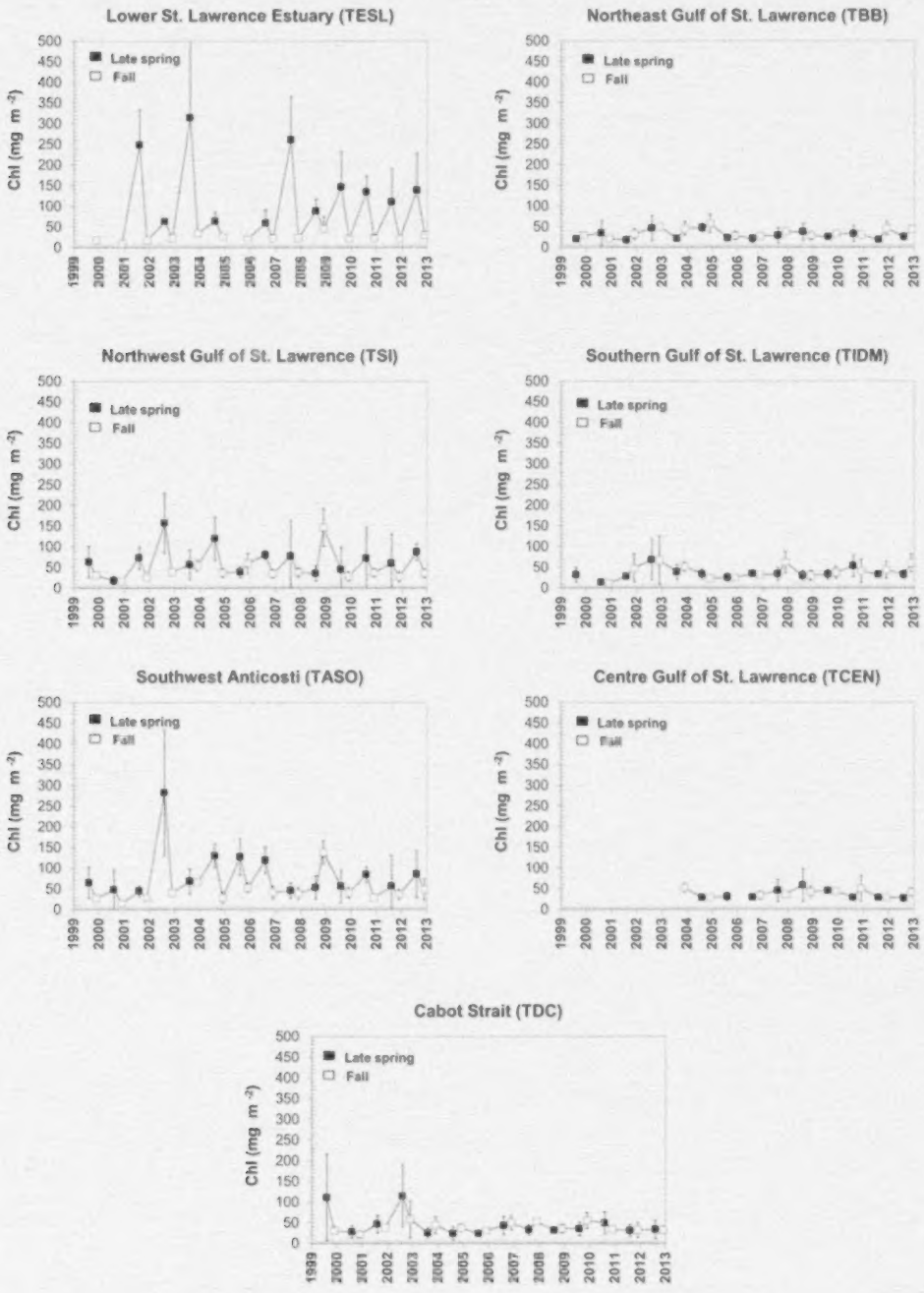
Lower St. Lawrence Estuary (TESL)
Northeast Gulf of St. Lawrence (TBB)
Northwest Gulf of St. Lawrence (TSI)
Southern Gulf of St. Lawrence (TIDM)
Southwest Anticosti (TASO)
Centre Gulf of St. Lawrence (TCEN)
Cabot Strait (TDC)
Late spring
Fall
Chl (mg m -2)

re 12. Time series of integrated (0–100 m) chlorophyll biomass along the seven AZMP sections from 9 to 2012.

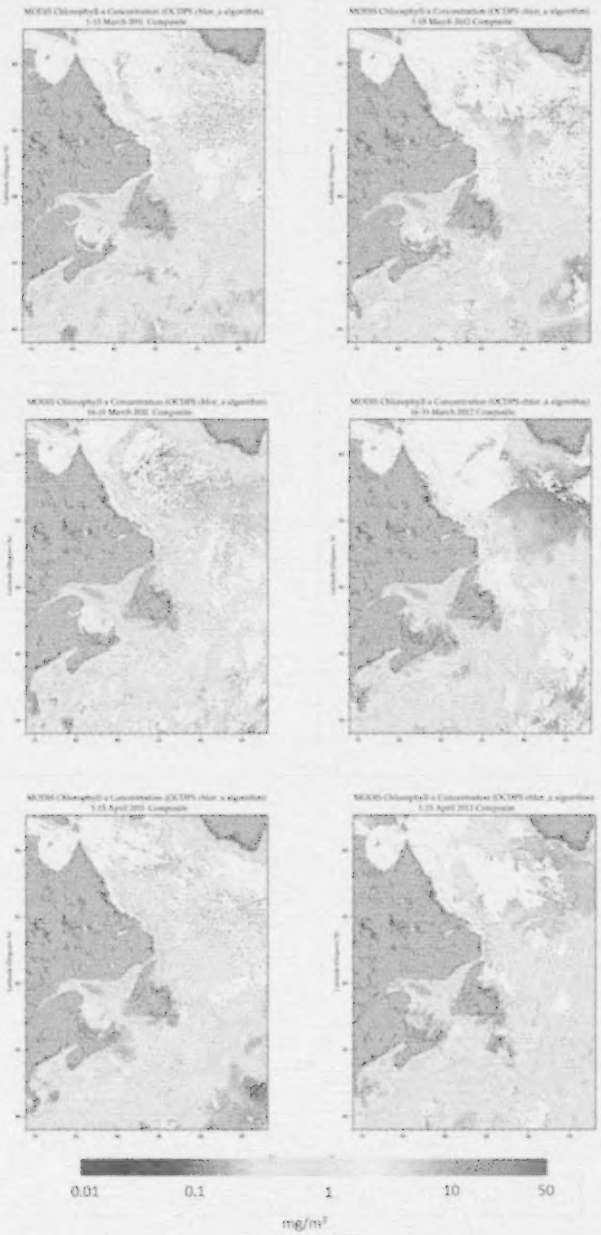

3. MODIS twice-monthly composite images of surface chlorophyll a in the Gulf of St. Lawrence te winter – early spring (1–15, 16–31 March; 1–15 April) 2011(left panels) and 2012 (right panel).

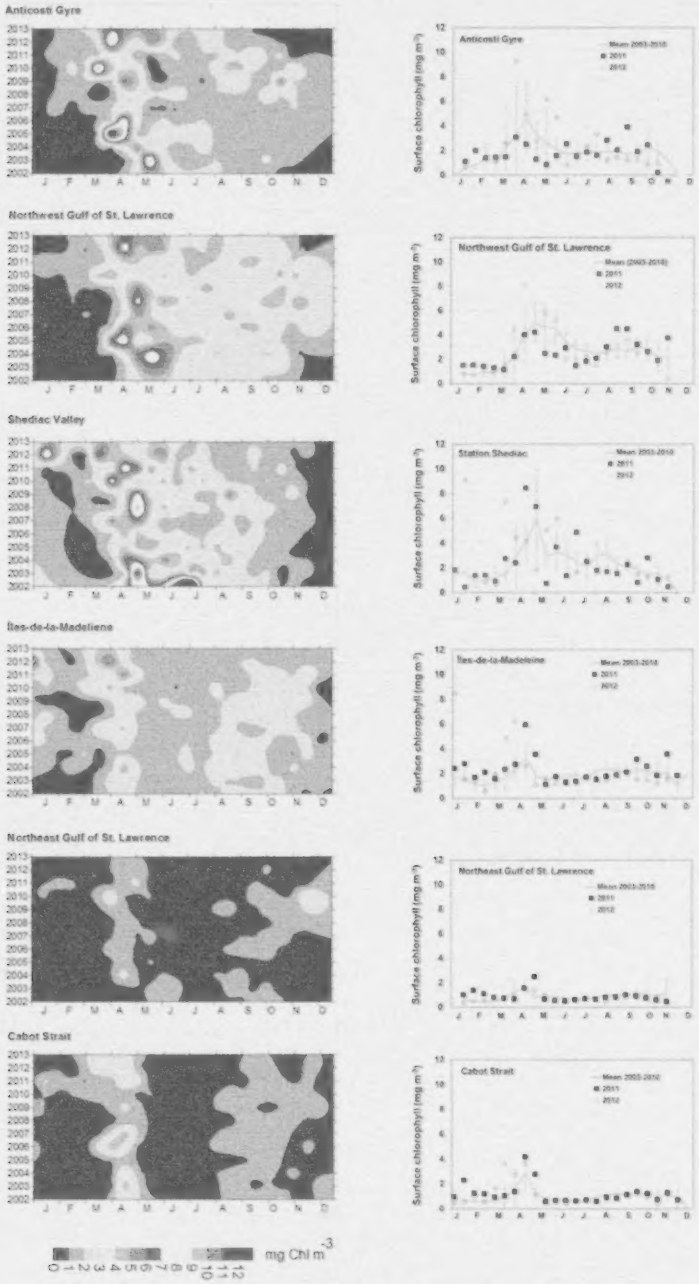

4. Left panels: Time-series of surface chlorophyll a concentrations from twice-monthly MODIS olour data in the Anticosti Gyre, Northwest Gulf of St. Lawrence, Shediac Valley, Magdalen s, Northeast Gulf of St. Lawrence, and Cabot Strait statistical subregions (see Fig. 3). Right comparison of 2011 (squares) and 2012 (circles) surface chlorophyll estimates from satellite olour with mean conditions from 2003–2010 (solid line) for the same statistical subregions.

es of change in productivity based on MODIS twice-monthly ocean colour composites

	Subregion	2002	2003	2004	2005	2006	2007	2008	2009	2010	2011	2012
Mean Surface Chl	Northwest Gulf of St. Lawrence		-0.69	0.24	1.24	-0.45	-1.82	1.15	0.30	0.03	-0.68	0.15
to December)	Anticosti Gyre		-0.51	-0.52	1.99	-0.49	-1.27	-0.25	0.38	0.68	-0.62	0.89
	Shediac Valley		-0.10	1.40	-1.07	-1.50	-0.53	1.04	0.34	0.41	-0.08	0.03
	Iles-de-la-Madeleine		-1.14	1.34	-1.19	-0.21	-0.01	-0.39	-1.81	0.09	-1.83	0.27
	Northeast Gulf of St. Lawrence		-0.40	0.14	-0.86	0.12	-0.14	-1.34	0.46	2.01	-0.59	-0.84
	Cabot Strait		-0.17	-0.32	-1.47	1.61	0.82	-0.84	-0.06	0.23	0.31	0.83
bloom magnitude	Northwest Gulf of St. Lawrence		-0.39	1.16	1.34	-0.20	-1.18	0.88	-0.50	-1.14	-1.97	1.08
	Anticosti Gyre		0.86	-0.36	0.60	0.54	-1.45	-1.33	-0.13	1.27	-1.35	0.77
	Shediac Valley		1.69	-0.20	-1.73	-0.72	-0.24	0.81	0.16	0.29	0.33	0.03
	Iles-de-la-Madeleine		-0.52	1.45	-1.50	-0.31	0.64	-0.77	-0.05	0.89	-0.15	2.73
	Northeast Gulf of St. Lawrence		-0.49	0.89	-0.51	-0.25	-0.08	-0.89	-0.76	2.07	0.59	-0.70
	Cabot Strait		1.01	0.26	-1.19	1.18	1.05	-1.10	-0.40	-0.80	0.53	0.21
urface Chl -	Northwest Gulf of St. Lawrence		-1.33	0.85	1.56	0.42	-1.20	-0.39	-0.34	0.44	-1.00	2.49
o May	Anticosti Gyre		-0.50	-0.37	2.06	-0.29	-0.93	-0.78	-0.06	0.84	-1.02	1.15
	Shediac Valley		0.43	0.68	-1.55	1.55	0.87	0.87	0.11	0.14	0.45	0.74
	Iles-de-la-Madeleine		-0.36	0.35	-1.17	-0.28	1.33	-1.31	0.09	1.34	2.08	2.47
	Northeast Gulf of St. Lawrence		-1.25	0.61	-0.53	0.34	0.19	-0.83	-0.47	1.53	0.76	0.29
	Cabot Strait		0.24	-0.18	-1.07	1.78	1.01	-1.16	-0.33	-0.30	0.92	1.79
urface Chl -	Northwest Gulf of St. Lawrence		0.47	0.67	1.43	-0.16	-1.68	0.66	-0.58	-0.81	-1.69	-1.07
August	Anticosti Gyre		-0.05	-0.09	1.98	-0.05	-1.50	0.59	-0.21	-0.67	0.28	0.99
	Shediac Valley		-0.11	-1.85	0.42	-0.74	-1.65	-0.16	0.22	0.17	-0.25	-0.46
	Iles-de-la-Madeleine		-0.47	1.92	0.29	0.48	-1.15	0.22	-0.09	-1.19	-1.14	-1.75
	Northeast Gulf of St. Lawrence		1.90	0.63	-0.08	-0.05	-0.65	-1.43	0.31	-0.64	-0.96	-1.30
	Cabot Strait		-0.41	-0.54	-1.58	1.72	0.54	-0.59	0.30	0.57	-1.12	-2.25
urface Chl -	Northwest Gulf of St. Lawrence	-2.03	-0.40	-1.02	-0.89	-0.90	-0.03	1.46	1.39	0.39	1.36	-0.97
ber to December	Anticosti Gyre	-2.11	-0.45	-0.66	-0.60	-1.11	-0.37	0.79	1.95	0.45	0.44	-1.70
	Shediac Valley	0.41	-0.74	-0.78	-1.13	0.17	-0.35	1.36	0.75	0.11	-0.98	-0.84
	Iles-de-la-Madeleine	-1.04	-0.90	0.21	-0.68	-0.33	-0.60	0.57	-2.17	-0.45	0.87	-1.07
	Northeast Gulf of St. Lawrence	-0.54	-0.78	-0.72	-0.89	-0.08	-0.02	-0.49	1.02	1.95	-1.12	-0.88
	Cabot Strait	1.23	-1.01	-0.38	-1.67	0.74	-0.10	0.45	0.53	1.42	-0.72	-0.76

es of change in seasonality based on MODIS twice-monthly ocean colour composites

	Subregion	2002	2003	2004	2005	2006	2007	2008	2009	2010	2011	2012
spring bloom	Northwest Gulf of St. Lawrence		0.76	0.76	0.00	0.00	0.00	0.76	0.00	-2.29	0.00	-0.76
	Anticosti Gyre		1.35	0.75	0.15	0.15	-1.05	0.75	-0.45	-1.65	-2.25	-1.65
	Shediac Valley		0.70	0.70	-0.90	0.70	-0.90	0.70	0.70	-1.70	-0.90	-0.90
	Iles-de-la-Madeleine		0.20	-1.37	-0.59	0.98	0.20	0.98	0.98	-1.37	0.20	-0.59
	Northeast Gulf of St. Lawrence		-1.58	0.00	0.00	1.58	0.00	0.00	-1.58	-3.16	0.00	-1.58
	Cabot Strait		0.98	0.20	0.20	-0.59	0.20	0.98	0.20	-2.15	-3.71	-1.37
of spring bloom peak	Northwest Gulf of St. Lawrence		1.21	1.21	-0.72	-0.72	0.24	0.24	0.24	-1.69	0.24	-0.72
	Anticosti Gyre		1.37	0.53	-0.32	-0.32	0.53	0.53	-0.32	-2.00	-1.16	-1.16
	Shediac Valley		0.78	-0.11	-1.89	-0.11	0.78	0.78	0.78	-1.00	-0.11	-1.89
	Iles-de-la-Madeleine		0.47	0.47	-2.34	0.47	0.47	0.47	0.47	-0.47	1.40	-0.47
	Northeast Gulf of St. Lawrence		2.31	-0.10	-0.10	-0.10	-0.10	-0.10	-0.90	-0.90	0.70	-0.10
	Cabot Strait		0.28	0.28	0.28	-0.85	0.28	1.41	0.28	-1.97	0.28	-1.97

Annual anomalies (scorecard) of chlorophyll biomass indices (means for various time periods agnitude of the spring bloom) and indices of seasonality (start and peak timing) of the spring kton bloom across Gulf of St. Lawrence statistical subregions (based on MODIS twice-monthly our composites) from 2002 to 2012. The reference period used to compute annual anomalies –2010. Blue colours indicate anomalies below the mean and reds are anomalies above the

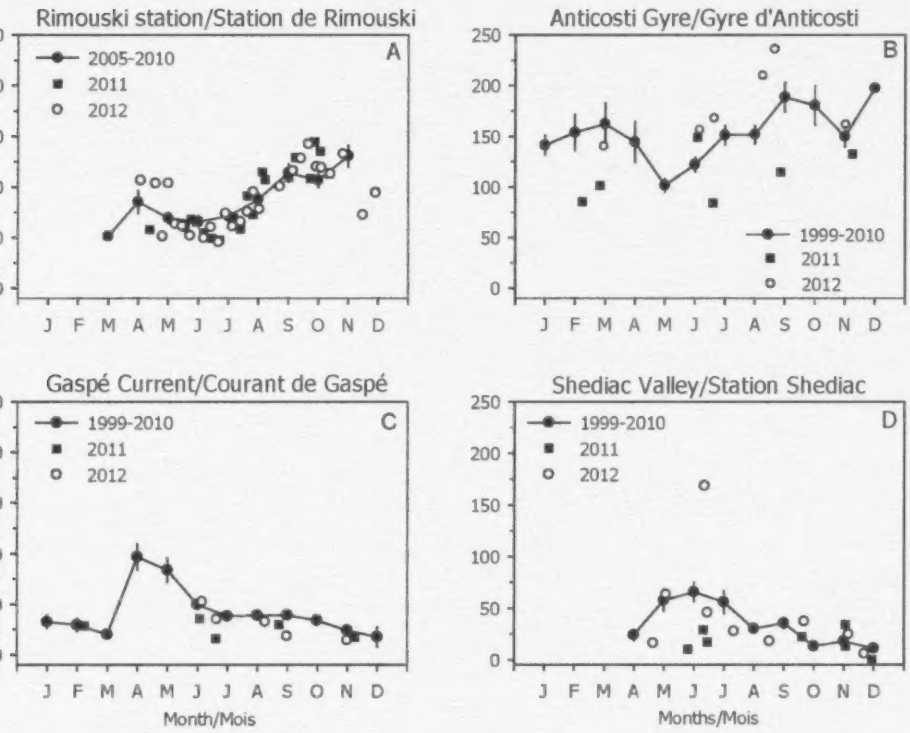

Comparison of total zooplankton biomass in 2011 (squares) and 2012 (circles) with the matology from 1999–2010 (Rimouski 2005–2010) (solid line) at the Gulf of St. Lawrence fixed ertical lines are standard errors of the annual averages.

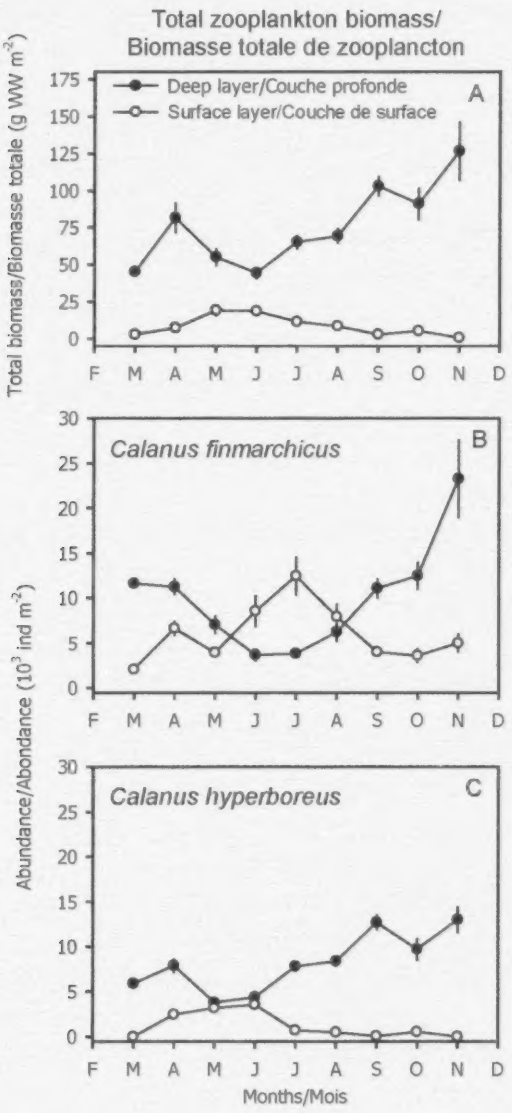

onthly climatologies of total zooplankton biomass (A) and total abundance of Calanus (B) and Calanus hyperboreus (C) in the surface (0–100 m) and deep (100–320 m) layers at ion from 2005 to 2010. Vertical lines are standard errors.

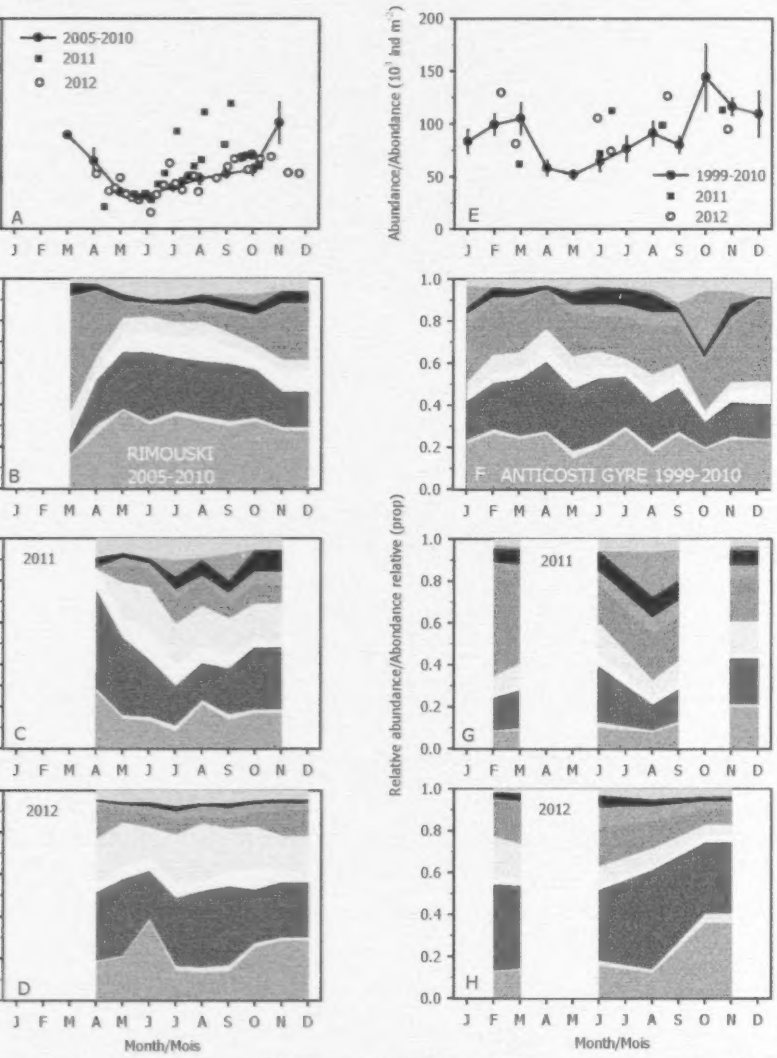

al variability in abundances of the 10 dominant copepod species at the Rimouski (left
sti Gyre (right panels) fixed stations. Climatologies of combined counts for the
are plotted with data from 2011 (squares) and 2012 (circles)(including the "others"
easonal variability by species for the reference periods (B, F), for 2011 (C, G), and for
so shown. Vertical bars in A, E are standard errors.

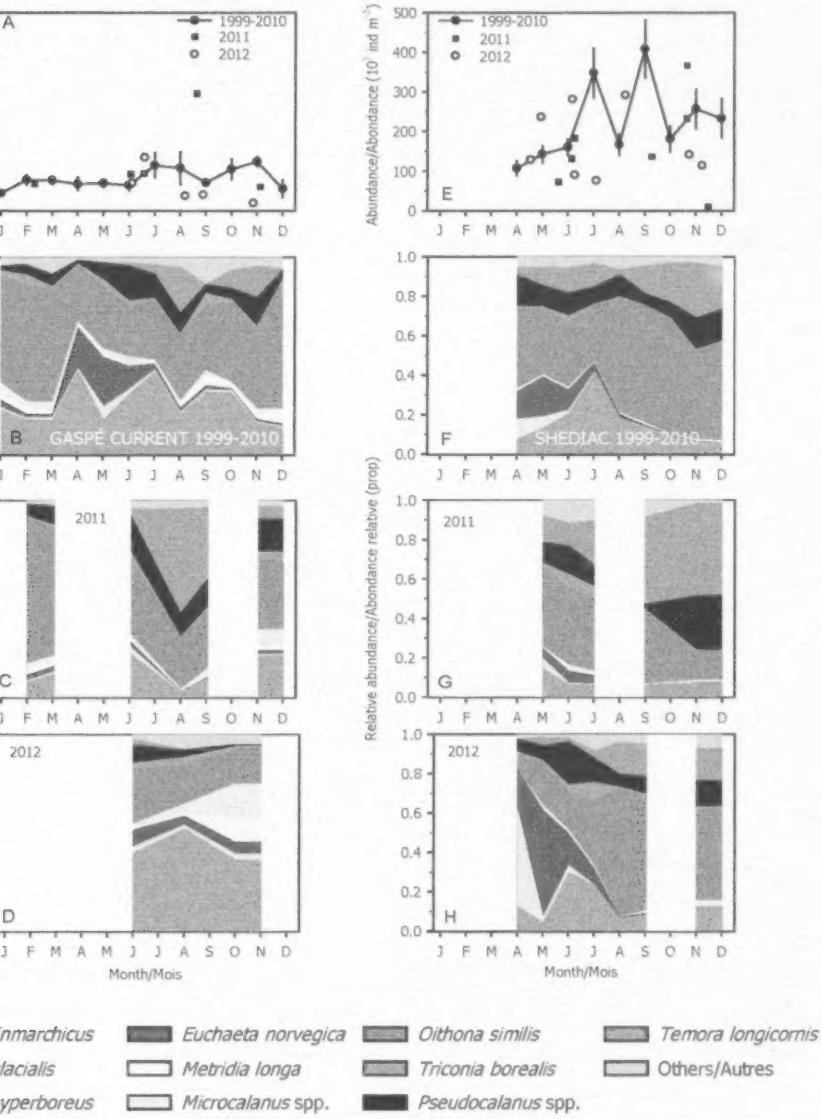

variability in abundances of the 10 dominant copepod species at the Gaspé Current
diac Valley (right panels) fixed stations. Climatologies of combined counts for the
plotted with data from 2011 (squares) and 2012 (circles) (including the "others"
sonal variability by species for the reference period (B, F), for 2011 (C, G), and for
shown. Vertical bars in A, E are standard errors.

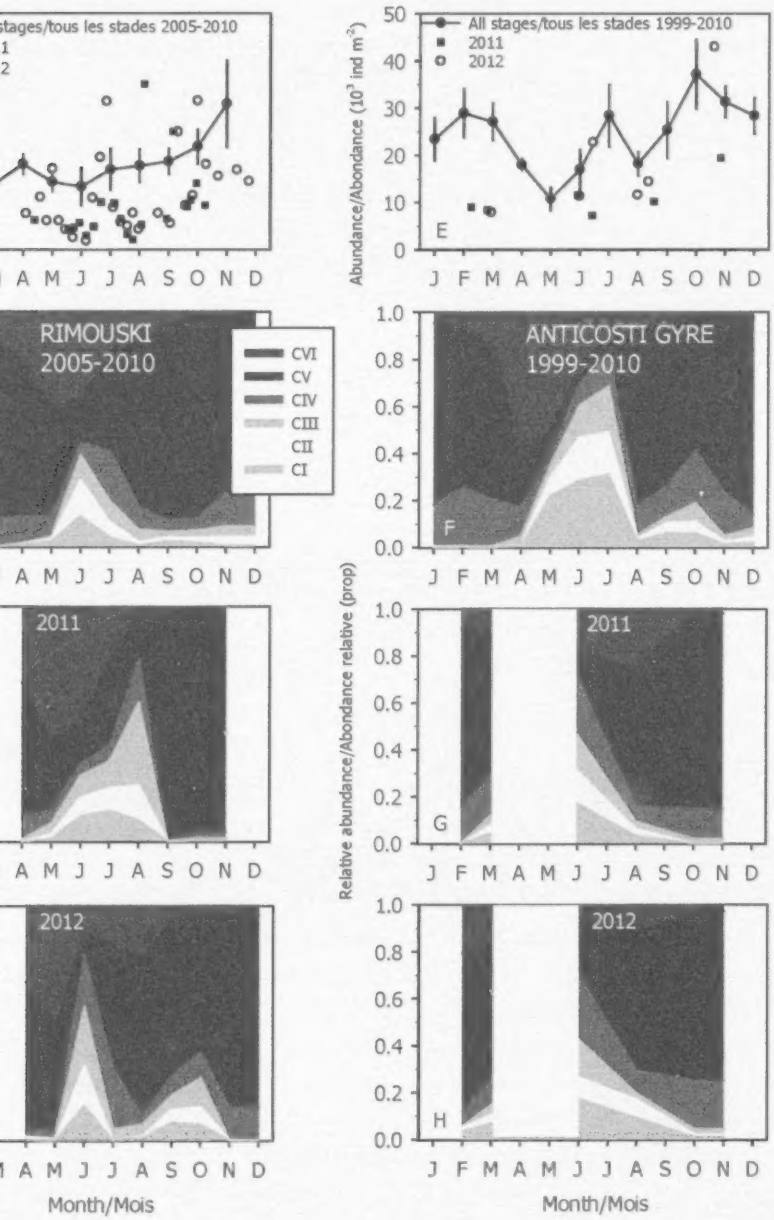

ariability in Calanus finmarchicus copepodite abundances at the Rimouski (left Gyre (right panels) fixed stations. Climatologies of combined counts for the plotted with data from 2011 (squares) and 2012 (circles) (A, E). Seasonal vidual copepodite stages for the reference periods (B, F), for 2011 (C, G), and for hown. Vertical bars in A, E are standard errors.

Abundance/Abondance (10^3 ind m^{-2})

Reiative abundance/Abondance relative (prop)

Figure 21. panels) an reference for the indi are also sh

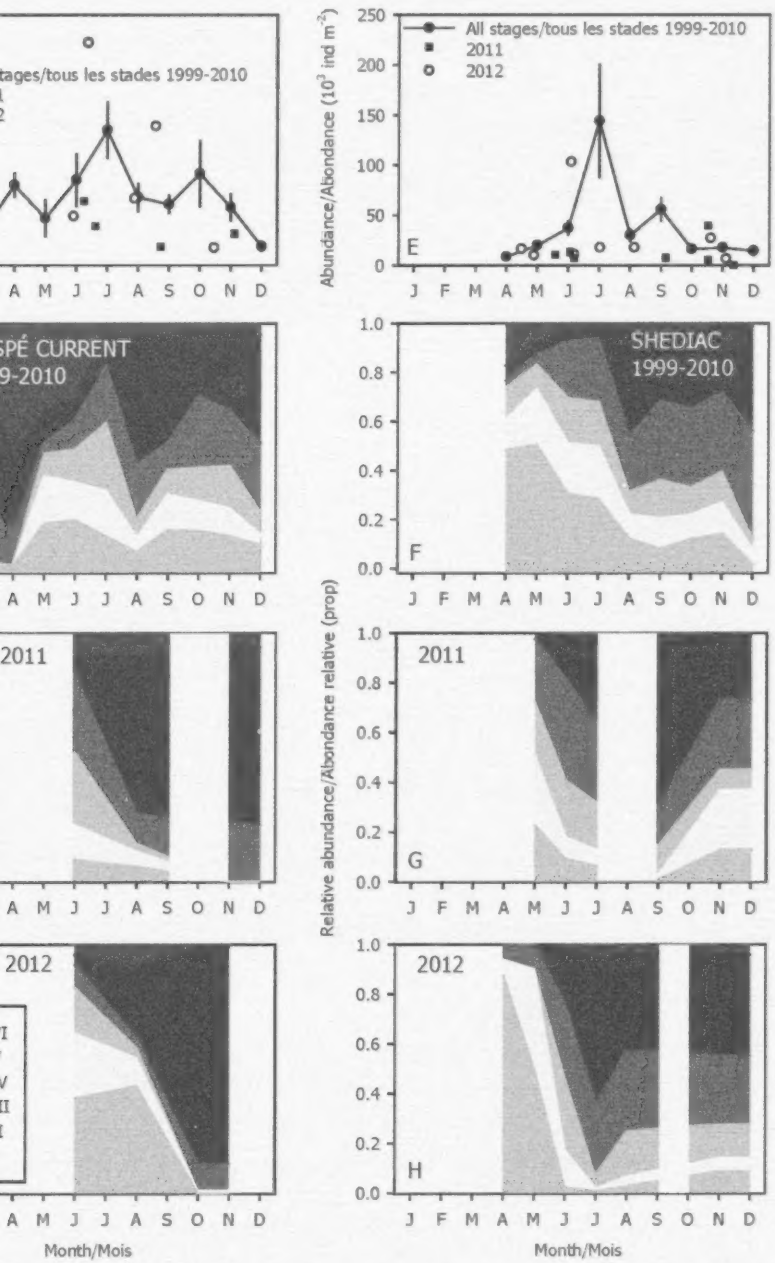

ility in Calanus finmarchicus copepodite abundances at the Gaspé Current (left ley (right panels) fixed stations. Climatologies of combined counts for the ted with data from 2011 (squares) and 2012 (circles) (A, E). Seasonal variability dite stages for the reference period (B, F), for 2011 (C, G), and for 2012 (D, H) bars in A, E are standard errors.

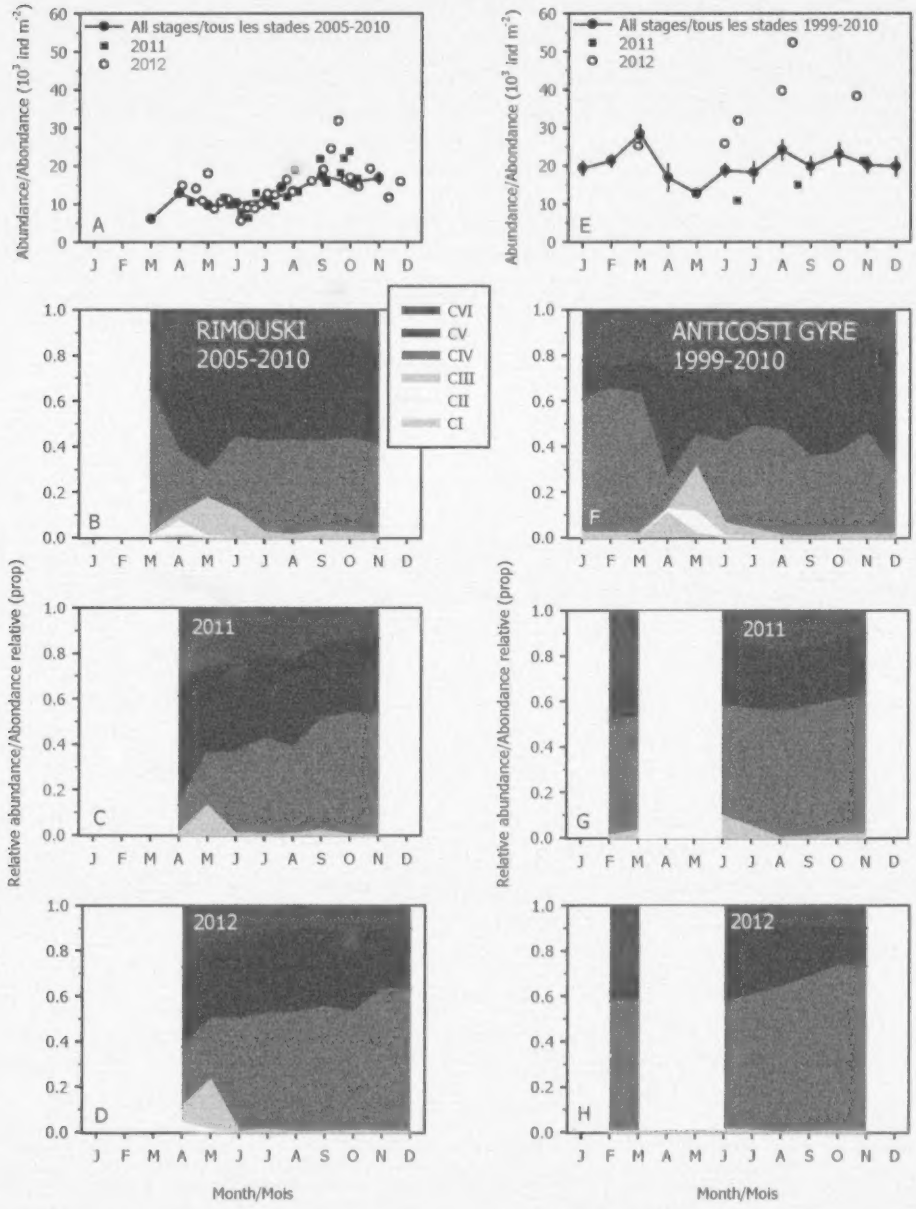

Figure 22. Season variability in Calanus hyperboreus copepodite abundances for the Rimouski (left panels) and Anticosti Gyre (right panels) fixed stations. Climatologies of combined counts for the reference periods are plotted with data from 2011 (squares) and 2012 (circles) (A, E). Seasonal variability for the individual copepodite stages for the reference periods (B, F), for 2011 (C, G), and for 2012 (D, H) are also shown. Vertical bars in A, E are standard errors.

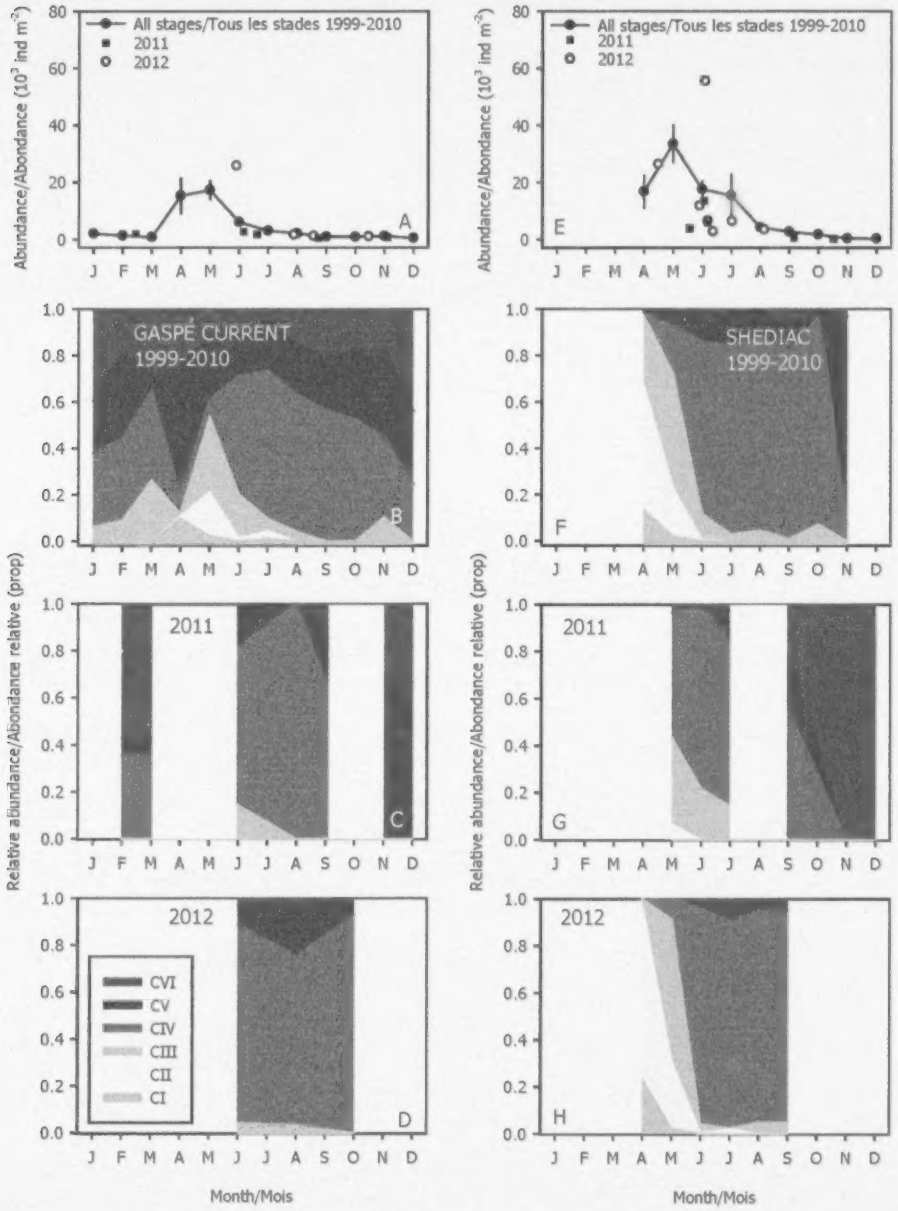

Figure 23. Season variability in Calanus hyperboreus copepodite abundances for the Gaspé Current (left panels) and Shediac Valley (right panels) fixed stations. Climatologies of combined counts for the reference period are plotted with data from 2011 (squares) and 2012 (circles) (A, E). Seasonal variability for the individual copepodite stages for the reference periods (B, F), for 2011 (C, G), and for 2012 (D, H) are also shown. Vertical bars in A, E are standard errors.

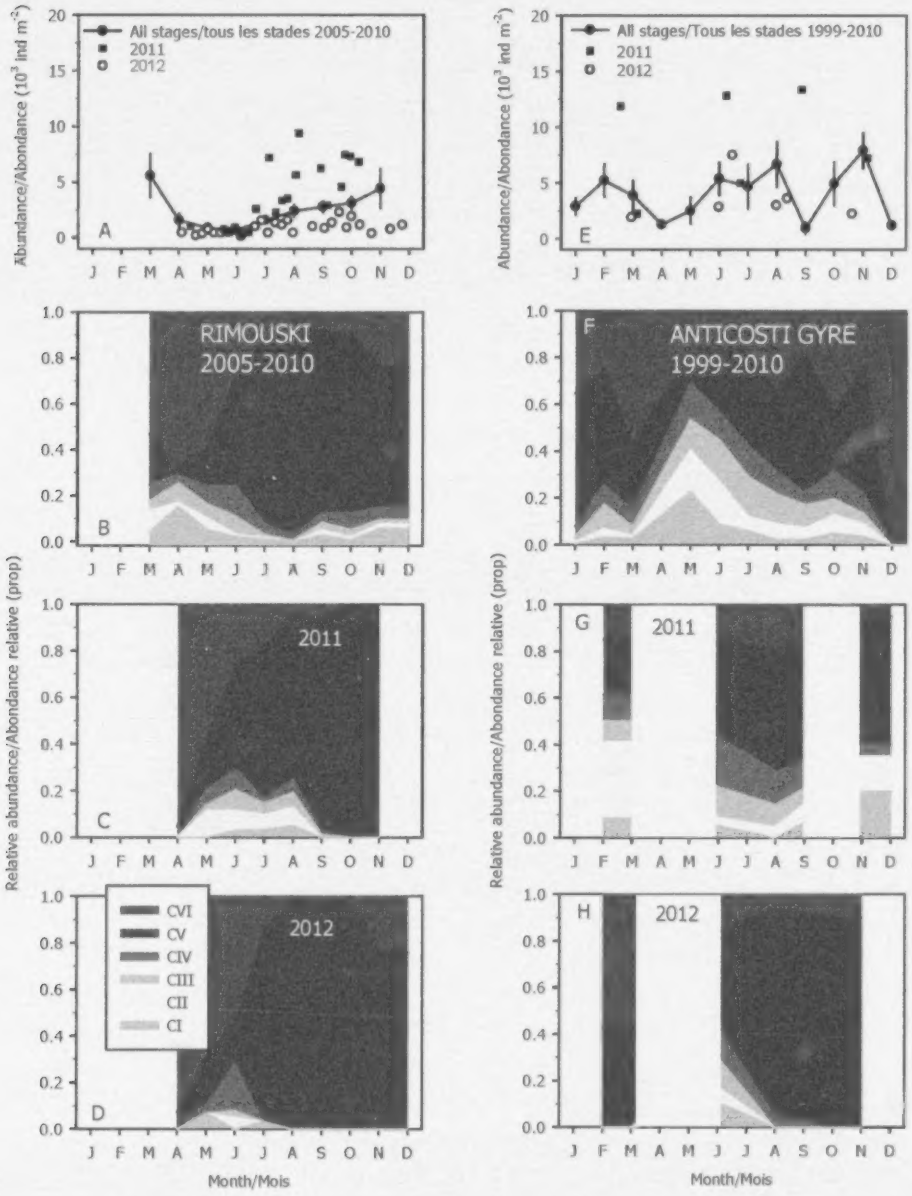

Figure 24. Season variability in Pseudocalanus spp. copepodite stage abundances for the Rimouski (left panels) and Anticosti Gyre (right panels) fixed stations. Climatologies of combined counts for the reference periods are plotted with data from 2011 (squares) and 2012 (circles) (A, E). Seasonal variability and for the individual copepodite stages for the reference periods (B, F), for 2011 (C, G), and for 2012 (D, H) are also shown. Vertical bars in A, E are standard errors.

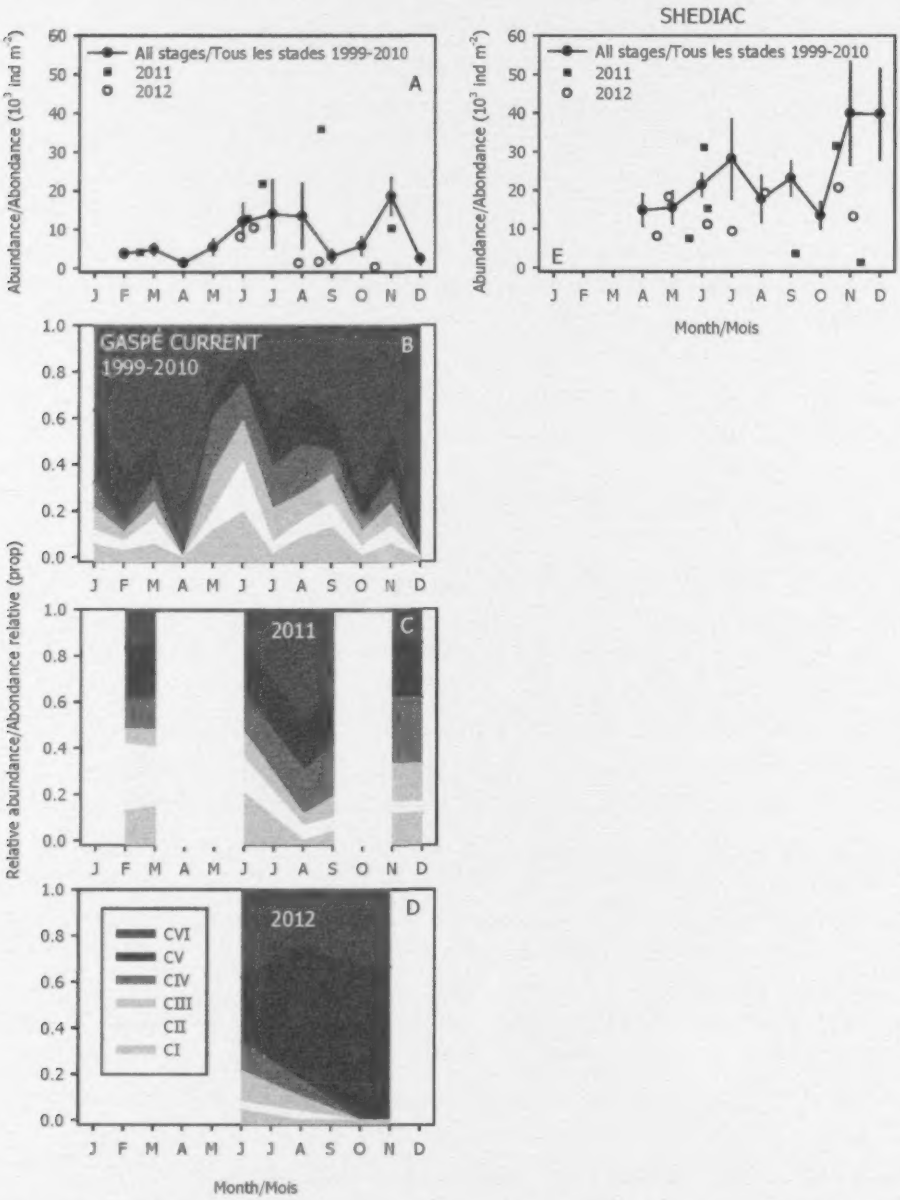

Figure 25. Season variability in Pseudocalanus spp. copepodite stage abundances for the Gaspé Current (left panels) and Shediac Valley (right panel) fixed stations. Climatologies of combined counts for the reference period are plotted with data from 2011 (squares) and 2012 (circles) (A, E). Seasonal variability for the individual copepodite stages for the reference period (B), for 2011 (C), and for 2012 (D) at the Gaspé Current are also shown; no stage information is available for Shediac Valley. Vertical bars in A, E are standard errors.

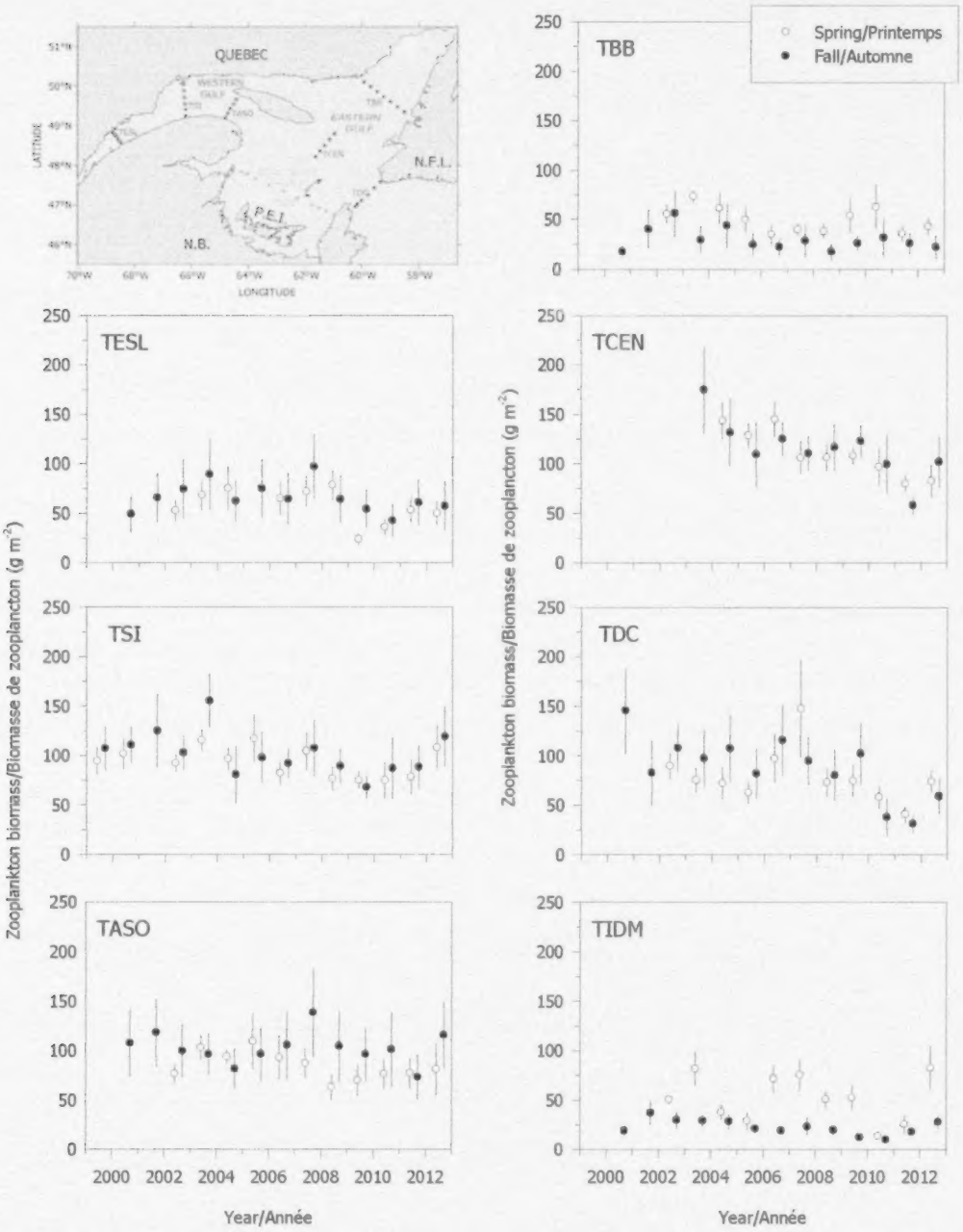

ure 26. Mean total zooplankton biomass for the seven Estuary and Gulf of St. Lawrence sections ing spring and fall from 1999 to 2012. Vertical bars represent standard errors.

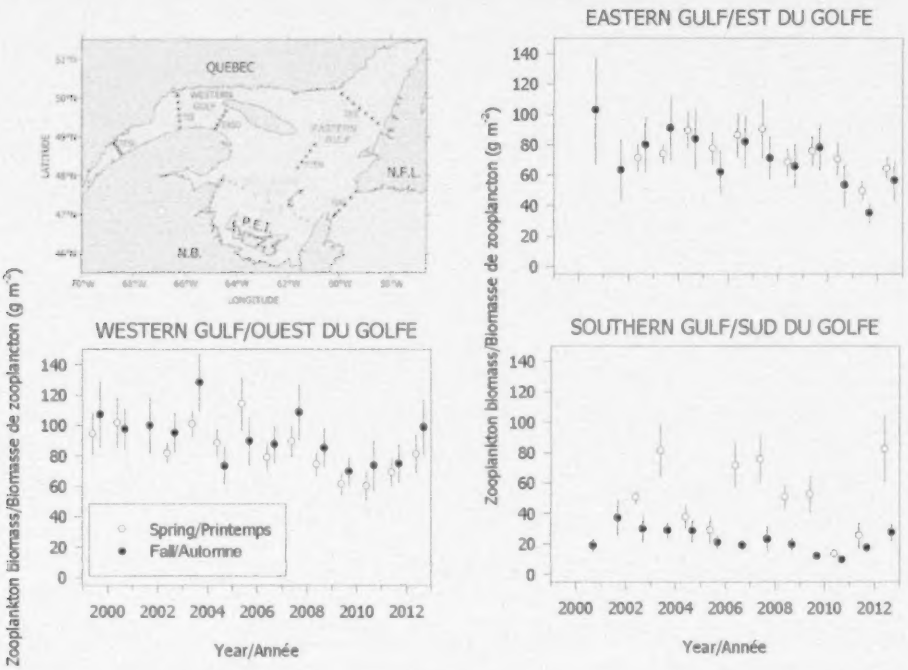

e 27. Mean total zooplankton biomass during spring and fall for three subregions of the Estuary and of St. Lawrence from 1999 to 2012. Vertical bars represent standard errors.

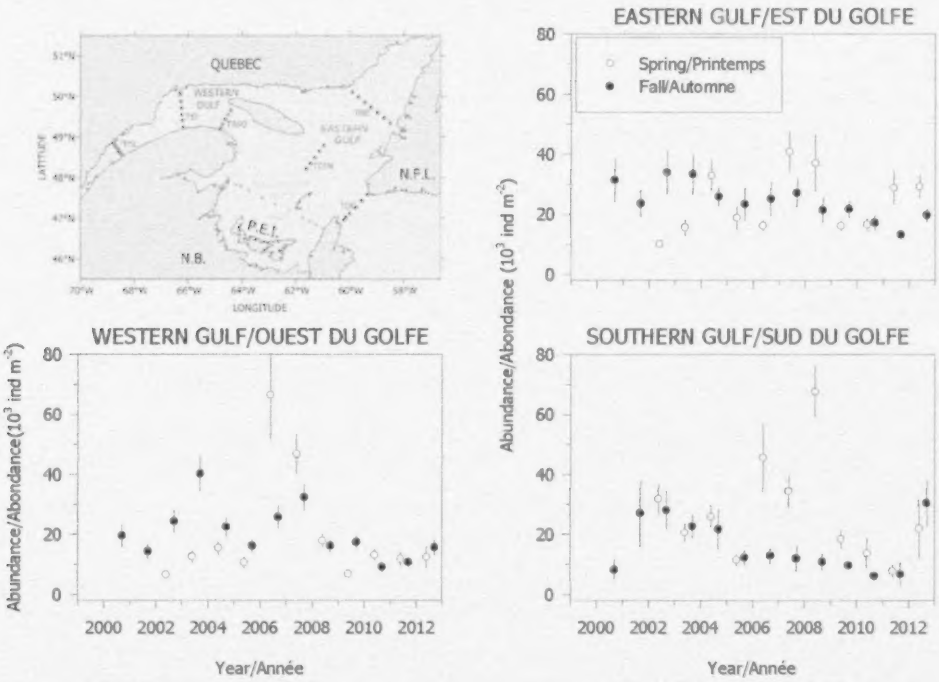

e 28. Mean total abundance of Calanus finmarchicus during spring and fall for three subregions of stuary and Gulf of St. Lawrence from 1999 to 2012. Vertical bars represent standard errors.

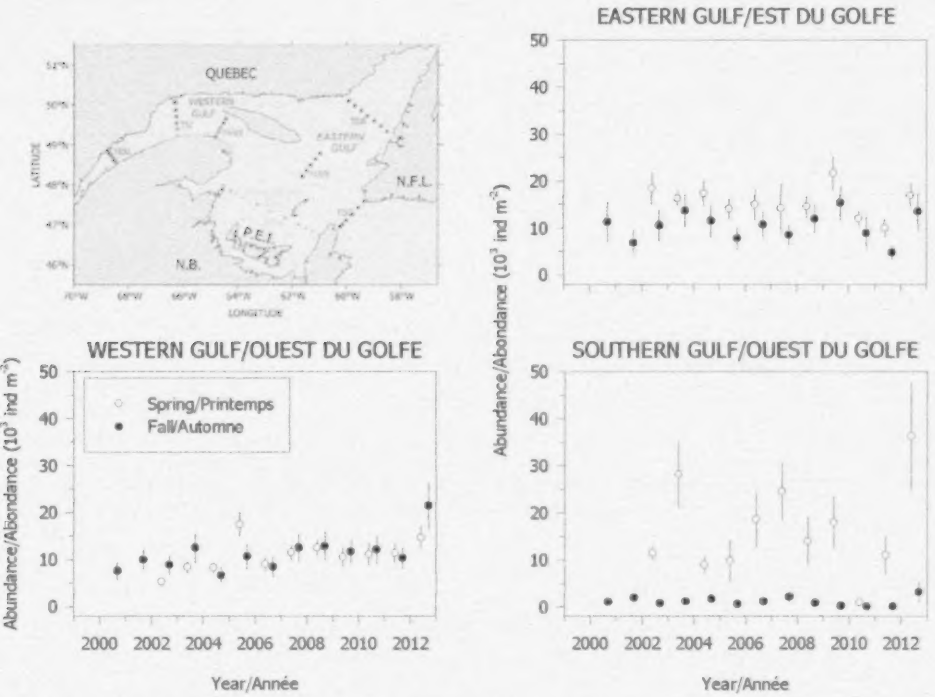

29. Mean total abundance of Calanus hyperboreus during spring and fall for three subregions of uary and Gulf of St. Lawrence from 1999 to 2012. Vertical bars represent standard errors.

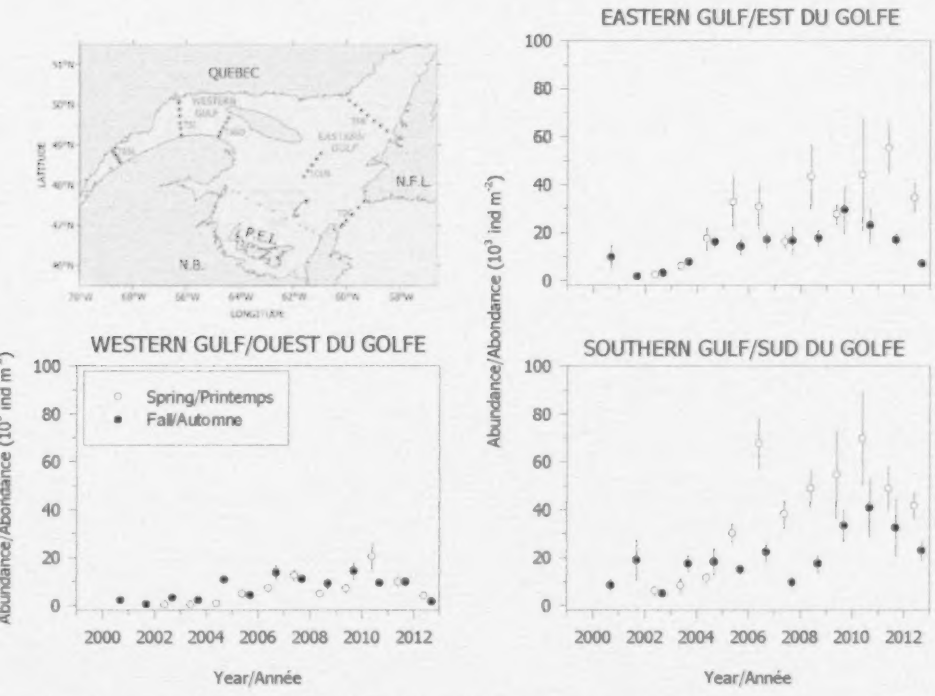

30. Mean total abundance of Pseudocalanus spp. during spring and fall for three subregions of the r and Gulf of St. Lawrence from 1999 to 2012. Vertical bars represent standard errors.

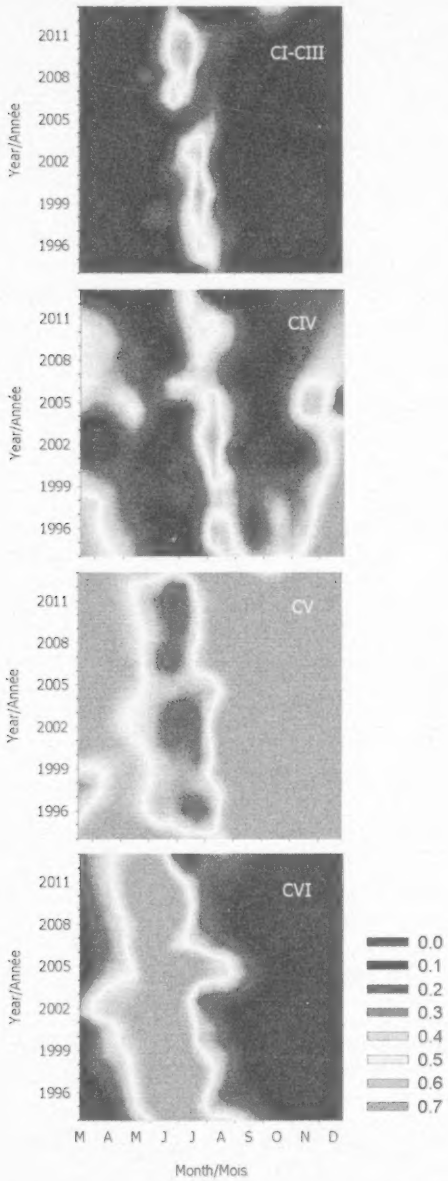

. Seasonal cycle in proportions (proportion of stage-specific annual maximum) of stage CI–III, CVI (male + female) Calanus finmarchicus copepodites from 1994 to 2012 at Rimouski station.

Regions	1999	2000	2001	2002	2003	2004	2005	2006	2007	2008	2009	2010	2011	2012
Rimouski							-1.01	-0.11		0.39	-0.08	-0.92	-0.66	-0.57
Gaspé Current	-0.41	-0.54		-0.03		0.12	-0.97	0.12	1.19	0.22	1.21	-1.09	-0.78	0.37
Anticosti Gyre	-1.12	-0.97	0.06	-0.83		1.35	-0.27	0.58	0.05	-0.08	-0.32	-0.74		-0.72
Shediac	-0.62	-0.21	-0.32	-0.44		1.27	-0.37	0.03	-0.14	0.12		-0.90	-1.29	-0.05
TESL		-0.07		0.16	0.42	0.04	-0.19	-0.20		-0.12	-0.70	-1.24	-1.10	-1.03
TSI		0.03	-0.26	-0.79	1.13	-0.12	-0.90		1.17	-0.56	-0.85	-0.86	-0.71	-0.66
TASO		-0.21	-0.63	-0.51	-0.03	-0.33	-0.54		1.04	-0.28	-0.63	-0.54	-0.67	-0.24
TIDM			0.54	0.86	-0.02	0.23	-1.04	0.80	0.14		-0.81			0.45
TCEN						-0.58	-0.62	-0.43	1.17	-0.05	-0.49	-0.92	-0.76	-0.02
TBB		-0.37	0.14	-0.59	-0.87	1.10	-0.10	-1.19	1.09		-0.71	-0.53	-0.27	0.50
TDC			-0.26	0.20	-0.22		-0.50	0.05	-0.31	-0.38	-0.98	-1.28	0.17	-0.78
wGSL		-0.16	-0.61	-0.51	0.47	-0.23	-0.63			-0.37	-0.80	-0.89	-0.87	-0.63
sGSL			0.54	0.86	-0.02	0.23	-1.04	0.80	0.14		-0.81	-1.08		0.45
eGSL		1.29	-0.18	-0.47	0.16	0.98	-0.66	-0.86	1.38	0.88	-1.06	-1.46	-0.61	0.00
Rimouski							-1.06	-0.79	0.69	-0.50	0.07			-0.94
Gaspé Current	-0.75	-0.67	-0.88	-0.86	-0.73	-0.57	-0.34	-0.14	0.45	0.99		2.01	0.58	-0.57
Anticosti Gyre	-0.90	-0.97	-0.89	-0.92	-0.82	0.14	-0.13	-0.17	0.39	0.79			0.71	-0.38
Shediac	1.34	-0.85		-0.07	-0.11	-0.96	0.42		-0.81	-0.31	0.12	0.81	0.98	-0.17
TESL		-0.64	-1.15	-1.15	-0.92	1.23	-0.64	1.42	1.28	-0.27	0.20	0.64	0.07	-0.80
TSI		-0.80	-0.99	-0.84	-0.97	-0.50	-0.41	0.56	0.71	0.02	1.17		0.31	-0.62
TASO		-0.83	-1.32	-0.76	-0.96	-0.47	-0.50	0.85		0.51	0.56	1.39		-0.67
TIDM		-1.02	-0.43	-1.18	-0.77	-0.68	-0.22	1.06	-0.14	0.39	1.00		0.81	0.34
TCEN					-1.23	-0.95	-1.36	0.66	0.29	0.80	0.90	0.88	4.20	1.33
TBB		-1.04	-1.12	-1.10	-0.86	-0.31	0.17	0.15	0.18	1.40		0.83	1.29	0.62
TDC		-0.71	-1.30	-1.19	-0.89	0.05	0.79	0.78	-0.41	0.77	0.22		1.35	-0.17
wGSL		-0.86	-1.20	-0.94	-1.04	-0.23	-0.38	0.83	1.10	0.11	0.88		0.71	-0.73
sGSL		-1.02	-0.43	-1.18	-0.77	-0.68	-0.22	1.06	-0.14	0.39	1.00		0.81	0.34
eGSL		-0.70	-1.41	-1.33	-0.95	-0.08	0.53	0.55	-0.12	1.12	0.96	1.43		0.27
Rimouski							-1.47	-0.62	1.14	-0.19	1.05	0.08	1.38	-0.10
Gaspé Current	1.14	-0.79	-1.34	-1.26	-0.19	-0.69	0.00	-0.52	0.06	1.35	0.60		0.26	-1.25
Anticosti Gyre		-1.37	-0.41		-0.05	0.38	0.10	-0.54	-0.66		0.43	0.34	-0.12	-0.37
Shediac	0.72	-0.95	-0.34	-0.72	1.24	0.03	-0.33	-0.99	0.69		-1.07	-0.41	-0.69	-0.85
TESL		-0.60	-1.00	-1.48	-1.14	-0.04	0.63	0.22		0.32	0.31	0.85	-0.77	
TSI		0.83	-0.43	-1.30	-1.18	-0.80	-0.83	0.82	0.18	0.79	0.08		-0.61	
TASO		-0.36	-1.22	-0.48	-1.01	-0.63	-0.60		-0.09	1.09	0.30	0.92	-0.21	-1.05
TIDM		-1.41	-0.19	0.67	-0.60	-0.47		0.76	-0.19		1.11	0.39	-0.07	0.16
TCEN						-0.69	-1.30	-0.68	0.00	-0.06	-0.21	1.43	0.39	-0.28
TBB			-1.45	-0.15	-0.66	1.41	-0.53	-1.33	0.10	0.49	0.41	-0.01	0.55	-0.38
TDC			-1.35	0.09	-0.27	0.50	-0.95	0.42	-0.68	0.79	-0.62	-0.22	0.50	
wGSL		-0.16	-0.99	-1.18	-1.28	-0.66	-0.37	1.37	0.58	0.95	0.27	1.48	-0.56	
sGSL		-1.41	-0.19	0.67	-0.60	-0.47		0.76	-0.19		1.11	0.39	-0.07	0.16
eGSL			-1.25	0.02	-0.21	0.58	-0.97	-0.74	-0.28	0.33	-0.20	0.22	0.41	-0.79
Rimouski							-0.93	-0.70	1.15	-0.97	0.31	1.13		-1.07
Gaspé Current	0.09	0.38	-1.04	-0.63	-0.38	-0.99	-0.77	-0.13			0.23	-0.56		-0.17
Anticosti Gyre	0.74	-0.25	-1.22	-0.96	-0.86	-1.04	-0.39	1.02		0.75	1.31	-0.62	0.95	-0.85
Shediac		-0.94	0.42	-0.26	-1.25	-0.79	1.04	0.24	0.27	1.34	-1.22	-0.55	-0.06	
TESL		-0.40	-0.56	-0.60	0.52	-0.52	-0.58	-0.09		-0.38	-0.17	-0.06	-0.23	-0.42
TSI		-0.69	-0.90	-0.74	-0.05	-0.70	-0.61		1.33	0.17	-0.25	0.11	1.45	-0.49
TASO		-0.56	-0.80	-0.66	-0.72	-0.67	-0.61	0.98		1.33	-0.06	-0.35	1.41	0.16
TIDM		-0.75	-0.89	-0.24	-0.65	-0.75	0.64	-0.20	0.02	0.06	0.11			1.39
TCEN						-0.03	0.29		0.86	-0.03	-0.67	-0.40	4.13	-0.36
TBB		1.27		0.32	-1.27	0.07	0.73	1.35	0.04	0.02	0.06	-0.61	6.87	0.87
TDC		-0.97	-1.42	-1.01	-0.81	0.14		0.87	0.89	-0.08	0.19	0.29		-0.87
wGSL		-0.65	-0.89	-0.77	-0.19	-0.75	-0.62	1.39		0.53	-0.18	-0.12	1.16	-0.28
sGSL		-0.75	-0.89	-0.24	-0.65	-0.75	0.64	-0.20	0.02	0.06	0.11			1.39
eGSL		-0.37		-0.63	-1.06	0.24		1.23	0.77	-0.02	0.07	-0.06	4.43	-0.35

Normalized annual anomalies (scorecard) for four zooplankton categories. Blue colours omalies below the mean and reds are anomalies above the mean.

	Regions	1999	2000	2001	2002	2003	2004	2005	2006	2007	2008	2009	2010	2011	2012
C. hyperboreus	Rimouski							0.81	-0.09	0.18	1.32	-1.27	-0.97	0.72	0.85
	Gaspé Current	0.10	-0.27	-1.79	-0.11	-1.03	-0.61	0.00	-0.40	-0.51	1.06	1.43	-1.20	-0.94	0.00
	Anticosti Gyre	-0.89	0.08	0.32	-1.54	0.14	0.23	1.26	-0.40	-0.26	-0.68	0.15	1.[illegible]	-0.89	3.48
	Shediac	0.16	0.76	-0.52	-1.32	1.15	-0.74	1.[illegible]	1.14	-0.14	-1.10	-0.73	-0.45	-1.13	-2.24
	TESL		-0.86	-0.19	-0.99	-0.09	-0.49	0.99	0.00	0.89	-2.53	-0.95	-0.54	0.49	[illegible]
	TSI		-0.78	-0.32	-1.33	1.33	-1.12	0.35	-1.02	0.62	0.49	0.15	[illegible]	1.07	5.15
	TASO		-0.91	0.25	-1.21	-0.54	-1.21	1.09	-0.70	0.61	0.10	[illegible]	0.71	-0.65	-2.71
	TIDM		-1.29	-1.05	-0.11	[illegible]	-0.24	-0.36	0.66	1.39	0.12	0.49	-1.32	-0.28	-2.76
	TCEN					0.16	0.58	0.01	-0.12	-1.59	0.29	[illegible]	-0.76	-1.05	-0.04
	TBB		-1.50	-1.02	1.10	1.21	1.20	-0.41	-0.75	-0.63	-0.64	0.84	0.59	-0.42	0.55
	TDC		0.31	-1.17	0.96	0.41	-0.52	-1.02	0.49	1.29	0.21	0.89	-1.85	-2.44	0.77
	wGSL		-1.20	-0.09	-1.42	0.15	-1.22	1.38	-0.67	0.83	1.15	0.43	0.67	0.31	3.70
	sGSL		-1.29	-1.05	-0.11	[illegible]	-0.24	-0.36	0.66	1.39	0.12	0.49	-1.32	-0.28	-2.76
	eGSL		-0.47	-1.94	0.59	0.71	0.66	-0.56	0.05	-0.41	0.19	[illegible]	-0.73	-1.73	0.83
Small calanoids	Rimouski							-0.86	-0.42	[illegible]	0.77	-0.34	-0.80	1.22	0.21
	Gaspé Current	-0.68	-0.79	-1.80	-0.72	0.39	-0.33	-0.80	0.26	0.60	[illegible]	[illegible]	0.39	1.18	-0.23
	Anticosti Gyre	-1.38	-0.97	-0.51	-1.57	0.43	0.48	0.18	0.10	0.03	[illegible]	0.51	0.91	-0.23	0.44
	Shediac	-0.91	-0.30	-0.85	-1.26	-2.48	0.96	0.53	0.38	-0.21	-0.12	-0.54	-0.13	0.40	1.24
	TESL		-0.54	-1.26	-0.82	-0.24	0.14	-0.21	0.46	2.61	0.40	-0.16	-0.36	-0.13	-0.15
	TSI		-0.65	-1.00	-1.37	0.04	-0.59	-0.88	[illegible]	1.05	0.62	0.20	0.70	0.17	-0.16
	TASO		-0.51	-0.90	-0.87	-0.48	-0.46	-0.53	-2.42	1.19	0.38	-0.13	-0.09	-0.14	-0.02
	TIDM		-1.68	-1.23	-0.17	0.41	-0.48	-0.81	1.26	-0.28	1.34	0.89	0.71	1.10	1.13
	TCEN					-2.24	-0.68	-0.96	-0.42	0.29	-0.04	0.13	-0.57	0.53	0.31
	TBB		-1.33	-1.22	-0.98	-0.50	[illegible]	-0.07	-0.46	0.19	1.40	0.91	0.38	1.34	0.79
	TDC		-0.12	-2.56	-0.33	0.41	0.80	0.37	0.63	-0.75	0.70	-0.10	0.95	1.41	-0.50
	wGSL		-0.66	-1.09	-1.12	-0.29	-0.44	-0.53	[illegible]	[illegible]	0.51	-0.02	0.14	-0.03	-0.12
	sGSL		-1.63	-1.23	-0.17	0.41	-0.48	-0.81	1.26	-0.28	1.34	0.89	0.71	1.10	1.13
	eGSL		-0.08	-2.46	-0.80	0.42	1.22	-0.08	-0.09	-0.15	1.10	0.51	0.40	[illegible]	0.32
Large calanoids	Rimouski							-0.22	-0.11	[illegible]	0.69	-0.83	-1.13	-0.10	-0.31
	Gaspé Current	-0.29	-0.50	-1.34	-0.12	[illegible]	-0.09	-0.95	0.09	0.92	0.31	1.27	-1.25	-1.04	0.21
	Anticosti Gyre	-0.93	-0.78	1.11	-1.51	[illegible]	1.36	0.39	0.20	-0.29	-0.64	-0.56	-0.13	-1.82	0.62
	Shediac	-0.38	0.03	-0.40	-0.85	2.59	0.82	0.37	0.38	-0.20	-0.30	-1.16	-0.90	-1.52	0.72
	TESL		0.30	-0.69	-0.03	-0.04	0.01	0.92	-0.21	-2.45	0.09	-1.16	-1.44	-1.12	-0.72
	TSI		-0.25	0.14	-0.90	1.37	-0.36	-0.81	[illegible]	1.26	-0.64	-1.06	-0.51	-0.51	0.18
	TASO		-0.38	-0.48	-0.62	-0.18	-0.58	-0.18	2.64	1.13	-0.36	-0.51	-0.48	-0.81	0.11
	TIDM		-1.58	0.14	0.60	0.63	0.04	-0.99	0.92	0.62	[illegible]	-0.51	-1.39	-1.38	[illegible]
	TCEN					-2.08	-0.41	-0.51	-0.52	0.54	-0.03	0.11	-1.28	-1.22	0.17
	TBB		-0.87	-0.53	-0.13	-0.43	[illegible]	-0.18	-1.66	0.95	[illegible]	-0.06	-0.21	-0.52	1.12
	TDC		[illegible]	-0.99	0.46	0.13	0.82	-0.96	0.33	0.80	-0.24	-0.15	-1.62	-0.86	0.06
	wGSL		-0.24	-0.41	-0.66	0.36	-0.48	-0.07	2.64	[illegible]	-0.39	-1.00	-0.87	-0.95	-0.11
	sGSL		-1.58	0.14	0.60	0.63	0.04	-0.99	0.92	0.62	[illegible]	-0.51	-1.39	-1.38	[illegible]
	eGSL		1.13	-1.35	-0.40	0.40	1.00	-0.69	-0.70	1.26	0.72	0.19	[illegible]	-1.22	0.81
Cyclopoids	Rimouski							-0.84	-0.71	-0.31	-0.66	1.45	1.07	0.14	-0.52
	Gaspé Current	0.18	-0.66	-2.36	-0.37	0.01	1.15	0.26	-0.72	-0.36	1.09	0.92	0.86	0.80	-1.21
	Anticosti Gyre	0.60	-1.06	-1.98	0.03	-0.51	[illegible]	-0.63	-0.01	-0.04	0.29	0.77	0.56	1.07	-0.50
	Shediac	-1.29	-1.29	-1.19	1.07	-0.82	1.23	-0.27	0.41	0.98	1.31	-0.04	-0.09	0.81	0.66
	TESL		-0.66	-1.98	0.18	-0.33	-2.01	0.38	-0.46	0.94	-0.10	0.35	-0.32	-0.89	-1.29
	TSI		0.43	-2.09	1.30	-0.75	1.10	-1.07	0.74	-0.04	-0.09	-0.02	0.49	-0.37	-1.14
	TASO		-0.46	-1.61	[illegible]	-0.59	0.98	-0.68	1.42	-0.45	-0.09	-0.18	-0.12	-0.48	-0.68
	TIDM		-0.76	-1.22	-2.61	-0.34	0.39	-0.85	0.23	-0.08	0.23	-0.14	-0.07	-0.53	-0.11
	TCEN					[illegible]	0.76	-1.50	-0.42	-0.27	-0.44	-0.21	0.17	0.53	-0.17
	TBB		-0.35	-1.37	[illegible]	-0.16	[illegible]	-0.65	-0.62	-0.17	-0.12	0.17	-0.45	-0.08	-0.24
	TDC		-0.28	-1.77	-2.23	-0.03	0.80	-0.98	0.06	-0.21	0.36	-0.13	-0.06	0.02	-0.75
	wGSL		-0.36	-2.09	1.37	-0.64	1.47	-0.64	0.80	0.10	-0.09	0.03	0.05	-0.61	-1.12
	sGSL		-0.76	-1.22	-2.61	-0.34	0.39	-0.85	0.23	-0.08	0.23	-0.14	-0.07	-0.53	-0.11
	eGSL		-0.15	-1.59	-2.29	0.10	1.24	-0.91	-0.35	-0.22	-0.04	-0.05	-0.23	0.03	-0.43
Copepod: warm species	Rimouski							-1.04	-0.91	1.41	-0.13	-0.32	0.99	[illegible]	0.32
	Gaspé Current	-0.72	0.39	-1.06	-0.99	-0.43	-0.66	-0.78	-0.49	0.86	[illegible]	0.48	[illegible]	6.02	3.06
	Anticosti Gyre	-0.74	0.01	-0.86	-0.73	-0.71	0.02	-0.78	-0.53	0.73	2.05	[illegible]	-0.20	[illegible]	-0.18
	Shediac	[illegible]	0.52	[illegible]	0.31	-0.36	-0.40	-0.29	-0.73	-1.21	-0.32	-0.86	-0.46	-0.99	0.35
	TESL		0.37	-0.90	-0.90	-0.90	-0.78	[illegible]	-0.61	[illegible]	0.07	-0.55	0.95	[illegible]	0.97
	TSI		0.29	-0.97	-0.97	-0.97	-0.71	-0.76	-0.42	0.87	[illegible]	1.29	0.63	[illegible]	0.41
	TASO		-0.46	-0.89	-0.81	-0.73	-0.81	-0.89	-0.17	0.64	[illegible]	0.95	1.46	3.24	1.05
	TIDM		-0.43	-0.57	-0.57	-0.42	-0.57	-0.51	-0.07	-0.45	-0.01	[illegible]	0.89	1.11	6.75
	TCEN					-0.69	-0.65	-0.54	[illegible]	-0.38	-0.39	0.41	-0.06	6.33	4.14
	TBB		0.11	-0.81	-0.84	-0.77	-0.64	[illegible]	-0.23	-0.67	[illegible]	0.71	-0.42	[illegible]	9.35
	TDC		0.24	-1.04	-0.82	-0.83	-1.01	0.51	0.08	-0.34	0.89	[illegible]	0.03	3.37	3.23
	wGSL		-0.09	-0.99	-0.96	-0.92	-0.82	-0.63	-0.36	0.99	[illegible]	1.02	1.12	[illegible]	0.79
	sGSL		-0.43	-0.57	-0.57	-0.42	-0.57	-0.51	-0.07	-0.45	-0.01	[illegible]	0.89	1.11	6.75
	eGSL		0.73	-1.11	-0.95	-0.96	-1.05	0.84	0.64	-0.57	0.89	[illegible]	-0.20	4.75	6.14
Copepod: cold species	Rimouski							-0.97	-1.00	0.28	-0.54	0.83	1.41	[illegible]	1.43
	Gaspé Current	-0.91	-0.91	-0.84	-0.84	-0.84	0.16	0.38	-0.16	-0.13	0.43	[illegible]	[illegible]	4.80	1.10
	Anticosti Gyre	-0.67	-0.68	-0.96	-0.93	-0.84	-0.45	-0.45	0.33	0.11	[illegible]	1.21	1.38	[illegible]	-0.54
	Shediac	-0.76	-0.66	-0.75	-0.94	-0.80	-0.25	-0.03	-0.09	0.10	[illegible]	0.76	0.89	0.93	-0.16
	TESL		-0.67	-1.22	-0.95	-1.00	-0.23	-0.65	1.39	0.92	[illegible]	0.36	0.62	1.11	-0.33
	TSI		1.22	-1.40	-1.14	-0.56	1.31	0.05	0.09	-0.08	1.09	1.29	0.59	[illegible]	0.68
	TASO		[illegible]	[illegible]	[illegible]	[illegible]	-1.05	-1.23	-0.02	-0.42	-0.25	0.11	1.28	[illegible]	0.97
	TIDM		-0.68	[illegible]	-0.55	0.36	0.36	0.68	0.48	[illegible]	0.72	0.00	[illegible]	[illegible]	-0.40
	TCEN					-0.97	0.42	-0.57	1.14	0.97	-0.06	1.04	1.21	1.00	0.36
	TBB		[illegible]	[illegible]	-0.47	0.19	-0.59	-0.51	1.07	[illegible]	0.88	1.22	1.40	[illegible]	0.68
	TDC		-0.78	-1.08	-0.97	[illegible]	-0.51	-0.50	1.03	0.34	1.22	0.96	1.40	0.65	-0.49
	wGSL		-0.52	[illegible]	-0.85	0.24	0.82	0.32	0.25	[illegible]	0.84	0.57	1.24	[illegible]	0.17
	sGSL		[illegible]	[illegible]	-0.47	0.19	-0.59	-0.51	1.07	[illegible]	0.88	1.22	1.40	[illegible]	0.68
	eGSL		-0.74	-1.23	-1.10	[illegible]	-0.24	-0.53	1.22	0.66	1.10	0.81	1.16	0.90	-0.29

Normalized annual anomalies (scorecard) for six categories of zooplankton assemblages. Blue icate anomalies below the mean and reds are anomalies above the mean.